EPRI

Rod Bundle Heat Transfer for Pressurized Water Reactors at Operating Conditions

Technical Report

DISCLAIMER OF WARRANTIES AND LIMITATION OF LIABILITIES

ORGANIZATION(S) THAT PREPARED THIS DOCUMENT

Virtual Technical Services, Inc.
Hughes and Associates

ORDERING INFORMATION

Requests for copies of this report should be directed to the EPRI Distribution Center, 207 Coggins Drive, P.O. Box 23205, Pleasant Hill, CA 94523, (800) 313-3774.

CITATIONS

This report was prepared by

Virtual Technical Services, Inc.
17000 Oak Leaf Drive
Morgan Hill, CA 95037

Principal Investigator
J. Harrison

Hughes and Associates
1330 Sioux Street
Los Alamos, NM 87544

Principal Investigator
D. Hughes

This report describes research sponsored by EPRI.

The report is a corporate document that should be cited in the literature in the following manner:

Rod Bundle Heat Transfer for PWRs at Operating Conditions, EPRI, Palo Alto, CA: 2000. 000000000001000215.

REPORT SUMMARY

Currently available heat transfer correlations for subcooled forced convection and subcooled boiling have not been validated with rod-array data at typical PWR fluid conditions. At the present time, rod bundle heat transfer processes cannot be analyzed with sufficient accuracy to make sound decisions regarding changes that might avoid an Axial Offset Anomaly (AOA).

Background

The axial offset anomaly first observed at the Callaway plant, and subsequently at numerous other pressurized water reactors (PWR), has called attention to the local thermal-hydraulic conditions in fuel rod bundles. From a thermal design and safety standpoint, there is little need to improve the fidelity of the rod bundle heat transfer model in the subcooled forced convection and subcooled boiling regimes. However, the ability to accurately model this region is important because of the sensitivity of deposition processes to the fluid temperature near the wall, the initiation of subcooled vapor generation, and the subcooled vapor generation rate.

Objectives

- To chart the course for the development, verification, and validation of improved thermal-hydraulic information.
- To report on published work of the state-of-the-art in rod bundle heat transfer that may be relevant to the PWR.
- To present the steps necessary, based on the literature review, for improving rod bundle thermal-hydraulic understanding as it pertains to PWRs.

Approach

There are several fundamental questions that summarize the unknowns: (1) Is there a solid experimental basis for the subcooled forced convection heat transfer coefficient at PWR operating conditions in an open lattice rod bundle geometry? (2) Is there a solid experimental basis for the superheat threshold for subcooled boiling at PWR operating conditions in an open lattice rod bundle geometry? (3) Is there a body of knowledge that qualifies the impact of typical PWR chemical additives on the heat transfer? (4) Can existing correlations be used to determine the vapor generation rate for bulk subcooled fluid flows in PWR cores at operating conditions?

To address these questions, a literature review was conducted covering rod bundle hydrodynamics and heat transfer. The literature reviews were organized into the following categories: historical reports and papers on which current heat transfer correlations are based; experimental investigations into rod-array turbulence, friction, and heat transfer; and other references of general interest.

Results

Some important results of the literature and model reviews included:

• The data on which the major correlation for the single-phase liquid heat transfer coefficient in rod bundles is based are significantly deficient relative to the bundle length, other geometric parameters, fluid conditions, and operating states.

• There are no heat transfer data in the open literature, either single-phase or boiling, available for the rod array geometry at typical PWR fluid conditions and chemical species.

• Application of standard engineering models of turbulent flow fields to the rod array geometry cannot be justified.

• No systematic experimental investigations of heat transfer in rod arrays at PWR steady state operating conditions have been reported in the open literature in about four decades.

In view of the above, an experimental program is required to obtain the necessary data to construct models of correlations for heat transfer in rod bundles. The experimental program should be performed with typical PWR geometry and grid designs, at PWR operating conditions, with typical chemical additives.

EPRI Perspective

This literature review has shown that there is no high fidelity data on which to base new heat transfer models for rod bundles. The only realistic way to improve the knowledge of heat transfer in PWR open lattice rod arrays is through prototypical testing. Performing a comprehensive test with top quality instrumentation can provide improved information which will allow the design and operation of fuel cycles with minimal economic impact from concerns of developing an adverse axial offset or deposits that may cause fuel failures. Acquiring such information through prototypical testing at the desired PWR operating conditions may present significant challenges to the researcher.

000000000001000215

Keywords

Axial offset anomaly
Deposition
Rod bundle heat transfer
Single-phase forced convection heat transfer
Subcooled vapor generation
Subcooled boiling heat transfer

EXECUTIVE SUMMARY

Important Conclusions

A review of the state-of-the-art for rod-bundle heat transfer, which may be important in the deposition processes on Pressurized Water Reactor (PWR) fuel rods, has shown the following:

- Significant uncertainties exist in the accuracy of all available correlations for the heat transfer processes important to deposition on PWR fuel rods.
- While there are significant uncertainties in the heat transfer correlations for subcooled forced convection or subcooled boiling, there are large margins to design limits. Therefore, there are no safety implications.
- None of the presently available heat transfer correlations for subcooled forced convection or subcooled boiling have been validated with rod-array data that includes fluid conditions typical of PWR operations.
- There are no heat transfer data in the open literature, either single-phase or boiling, available for the rod array geometry at typical PWR fluid conditions and chemical species.
- At the present time, rod bundle heat transfer processes cannot be analyzed with sufficient accuracy to make sound decisions regarding core design changes that might avoid deposition and the development of an Axial Offset Anomaly (AOA).
- Heat transfer data and correlations in the presence of typical PWR operating chemicals are not available. Data and correlations applicable to the clad surface after deposition has changed the surface characteristics are also not available.
- In view of the above, an experimental program is required to obtain the necessary data to construct models and correlations for heat transfer in rod bundles at typical PWR operating conditions. However, measuring the necessary heater rod and subchannel parameters in a rod array geometry at PWR pressures and temperatures is a difficult proposition. Therefore, an early assessment of the uncertainties in the experimental data will be important to determine if a realistic improvement in the scatter and uncertainties can be expected.

Introduction

The heat transfer processes of interest in a PWR core include:

- Heating of a single-phase subcooled liquid,
- Superheating of a thin liquid region adjacent to the fuel rod clad and nucleation of vapor in cavities on the fuel rod clad surface; onset of nucleation,

- Departure of the vapor bubbles from the clad surface; fully developed subcooled boiling, and
- Bulk boiling of the liquid as the fluid reaches the saturation temperature.

The literature has been reviewed to establish the state-of-the-art for modeling and correlating these processes in the PWR rod-array geometry. The rod-array geometry factor is one major focus of the review because it is significantly different from the typical tube or annulus used in the development of the vast majority of heat transfer test data. Experimental data for the rod-array geometry are only available for heating of single-phase liquid. The available data are severely limited relative to the geometries and operating states of interest for PWRs. No validated models and correlations for any of the other processes for the rod-array geometry have been found. Additionally, the onset of nucleation and subcooled boiling heat transfer mechanisms listed above are understood, at best, at an empirical engineering-level basis.

The impact of typical PWR chemistry on the heat transfer coefficient in the relevant heat transfer regimes has been studied only superficially. These studies noted some significant differences in the subcooled forced convection coefficient and void fraction in the presence of boric acid and lithium hydroxide. However, no experimental studies have been conducted at typical PWR operating conditions.

Single-Phase Liquid Heat Transfer

The heat transfer coefficient for heating of subcooled liquid determines the axial location where the clad-surface temperature reaches the saturation temperature. From this axial location onward downstream, the potential for nucleation and vapor generation exists. An accurate determination of this location may be important to control deposition processes that lead to the AOA problem.

No experimental data has been located for the heating of a single-phase liquid that cover the range of operating states (pressure, flow rate, and wall heat flux) in a PWR rod-array geometry. Generally, the available data are for Reynolds number less than that encountered in operating PWRs. Additionally, the available data do not cover the range of Prandtl number because the pressure and temperature ranges do not correspond to operating PWR conditions. Furthermore, all of the rod-array tests that have been conducted have used quite short test sections, making it difficult to be confident that bulk flow redistribution and entrance effects are not distorting the data.

Correlations for the heat transfer coefficient under single-phase flow conditions show significant differences in the dependency of the heat transfer coefficient on both the Reynolds and Prandtl number. The differences are of such a magnitude that, for typical PWR conditions, some will predict that the wall reaches the saturation temperature and others will predict that the wall does not reach that temperature. None of the existing correlations have been validated for heat transfer in rod-array geometries at PWR operating states.

In summary, at the present time there is no sound experimental basis for determination of the location at which the rod wall temperature reaches the saturation temperature in the rod-array geometry and at PWR operating states.

Boiling Heat Transfer Regimes

The generation of vapor at the cladding surface is deemed to be an important factor in processes that lead to the AOA problem. When nucleation begins on the rod surface in the subcooled environment, species may be concentrated and deposited. When nucleation begins, only a portion of the rod surface will be nucleating while the forced convection will continue elsewhere. The key information which is needed for deposition considerations is the portion of the heat flux that results in vapor generation. Heat transfer models are not concerned with this term separately. Interest in subcooled void fraction and its impact on power distribution and reactivity has led to the development of models which represent the vapor generation term after an observable void fraction is present. However, these models do not validate the generation term alone, only the net of the generation and condensation.

The important conclusions from the review of models and correlations for the onset of nucleation, partial subcooled boiling, and fully developed subcooled boiling are as follows:

- There are no experimental data from rod bundles that can be used to validate models and correlations for any of these heat transfer regimes,
- Available models and correlations for onset of nucleation and partial subcooled boiling are based on hypothetical mechanisms and assumptions which can not be directly validated,
- Models and correlations for the heat transfer coefficient for partial and fully developed subcooled boiling are especially limited relative to the ranges of geometries and operating conditions covered by experimental data; no correlations have been developed for the rod bundle geometry or at PWR operating conditions.

In Section 5, calculations with some of the available models and correlations suggest that onset of nucleation requires very little wall superheat at typical PWR operating conditions. Thus steaming can be expected when the clad surface temperature is only slightly superheated.

An experimental investigation of a rod-array bundle heat transfer under onset of nucleation, partial subcooled boiling, and fully developed subcooled boiling conditions will be necessary to develop and validate models for these heat transfer regimes. The determination of the onset of nucleation can probably be determined with conventional temperature measurement devices. However, the vapor generation rate may be determined only visually. Given the rod-array geometry and high operating pressure, it may be extremely difficult to observe the bubble growth into the subcooled fluid immediately after the onset of nucleation. The rod geometry will make it difficult to make a clean observation, and bubbles at PWR operating pressures will be quite small.

CONTENTS

LIST OF FIGURES

1
INTRODUCTION

Background

The axial offset anomaly (AOA) first observed at the Callaway plant and subsequently observed at numerous other pressurized water reactors (PWR) causes a variety of plant and core operating problems. A temporary reduction in power has been a result in some extreme AOA cases. The axial offset anomaly is the result of boron coming out of solution and depositing on fuel rods in the upper half of the core which depresses the neutron flux in this region. Significant studies have been performed to characterize the cause of the problem, as reported in *Rootcause Investigation of Axial Power Offset Anomaly* [1.1]. This work concludes that three conditions are required to cause the anomaly to develop:

- Soluble boron in the coolant, so that boron can be concentrated in the crud,
- Subcooled boiling to the extent necessary to concentrate the boron, and
- Crud deposits of sufficient thickness to serve as the porous medium for the $LiBO_x$ deposition.

Recommendations from this report focused on chemistry controls to limit the source terms for the crud which is the precursor required for the boron deposition.

Because boron and subcooled boiling are deemed necessary elements of the deposition process, researchers investigated methods to define the envelope of conditions where an AOA is likely to develop. Then, through core nuclear and thermal design modifications, this envelope could be avoided. The guidelines in *Thermal-Hydraulic Bases for Fuel Cycle Designs to Prevent Axial Offset Anomalies* [1.2] were the result of these studies. These guidelines provide an engineering level solution based on empirical observations at a number of plants. The guidelines do not include fundamental information about the processes which lead to an AOA problem. Such fundamental information would allow simulation of the evolution of AOA and a quantification of the margin to significant AOA problems.

Some of the fresh fuel in Three Mile Island Unit 1 (TMI-1) experienced localized cladding corrosion damage during Cycle 10. [1.3] The damage was characterized by a distinctive corrosion pattern between the fifth and seventh intermediate fuel rod spacer grids. The abnormal conditions appeared predominantly at the interface between neighboring fresh fuel assemblies and corner locations in fresh fuel assemblies. The damage was isolated to surfaces facing toward the gap between fuel assemblies.

Differences between the power distribution predictions and measurements were observed during TMI-1 Cycle 10. These differences were attributed to boron deposition on the fuel rods depressing the power in the upper half of the core; in other words, an AOA. Framatome Cogema

Fuels (FCF) performed extensive thermal-hydraulic analyses of the TMI-1 Cycle 10 core to search for factors which may have contributed to the formation of the crud and the cladding degradation. None of the FCF analytical examinations produced cladding surface temperatures at or above the coolant saturation temperature and thus indicated that subcooled boiling did not occur in the core. However, independent analysis performed by EPRI indicated surface temperatures may have reached saturation when a more conservative subcooled forced convection heat transfer coefficient was used.

The AOA in general, as well as the TMI-1 Cycle 10 fuel failure problem, are a result of both thermal-hydraulic and chemical conditions being present to produce the precursor crud and concentrate the boron from the coolant.

Fundamental Questions

The physical phenomena responsible for deposition include both thermal-hydraulic and chemical processes. The deposition processes depend on "local" thermal-hydraulic conditions: the microscopic velocity, temperature, and concentration distributions in the fluid, and the surface temperature of the fuel cladding. The heat transfer models which may have a bearing on these processes include:

- The heat transfer coefficient for forced convection to single phase subcooled liquid,
- The threshold of wall superheat required for the initiation of subcooled boiling, and
- The portion of the heat flux removed by nucleation during subcooled boiling.

The heat transfer coefficient models for these processes are difficult, but they are reasonably well understood in tubes. However, the models are complicated by the rod bundle geometry as well as other factors in the reactor core. In addition to the channel heat transfer characteristics, the axial and cross-flow velocity and temperature distribution is complicated in a rod bundle geometry and the fuel rod spacer grids. The partitioning of the heat flux between subcooled forced convection and nucleation is not well defined for most any fluid conditions, much less forced flow high pressure and temperature conditions.

For thermal design and safety analysis, the current state-of-the-art of the models listed above is quite acceptable. In other words, relatively large errors in the heat transfer correlations will have little impact on the approach to limiting design criteria. These models and correlations are discussed in some detail in Section 5.

However, because the deposition processes are sensitive to the fluid temperature near the wall and the subcooled vapor generation rate, the heat transfer coefficient and subcooled boiling correlations are quite important to the chemical deposition processes. A brief summary of the status of these correlations is given in the following paragraphs.

Subcooled Forced Convection and the Superheat Threshold for Subcooled Boiling. The temperature increase from the bulk fluid to the wall surface in subcooled forced convection is typically much larger than the wall superheat threshold above saturation needed for the initiation of boiling. Both processes and associated models are discussed in Sections 3 and 5. As shown in

Section 5, the more important question involves the forced convection heat transfer coefficient in a rod bundle geometry.

The difference between the FCF and EPRI predictions of the TMI core thermal-hydraulic conditions illustrates the potential range of uncertainty in predicting the threshold of subcooled boiling. Using the Weisman correlation [1.4] for the rod bundle subcooled forced convection heat transfer, FCF concluded that the cladding surface temperature could not reach the saturation temperature. In contrast, EPRI found that when using the default Dittus-Boelter model, the cladding did reach the saturation temperature. The Weisman correlation suggests that the leading coefficient to the Colburn equation should be larger, about 0.03, than the Dittus-Boelter value of 0.023 when applied to rod bundles. The difference in wall temperature for these two different predictions is approximately 4.4°C (8°F). Weisman's correlation is based, to a large degree, on data for square pitch rod arrays from Dingee, et al. [1.5]

Impact of Chemicals on the Heat Transfer Coefficient. There is very little known about the impact of boric acid and chemicals used for pH control on the subcooled single phase forced convection heat transfer coefficient, the wall superheat threshold for subcooled boiling, and the heat transfer coefficients for subcooled and saturated boiling. Staub, et al. [1.6] observed that the subcooled convection heat transfer coefficient for low mass velocities was significantly reduced when both pH control chemicals and boric acid were present. Staub also noted that the void fraction was significantly increased when these chemicals were present. While Staub’s work was limited to 6.89 MPa (1000 psia) and not exhaustive in terms of other parameter ranges, it is an important observation. Staub concluded that more work was needed in this area. It appears that no follow-on work has been performed to examine the impact of chemicals at PWR operating conditions.

Vapor Generation Rate. There are a variety of models which have been developed and used to predict subcooled and saturated boiling heat transfer. They each have slightly different characteristics and different developmental databases. The amount of vapor generated in subcooled boiling at PWR operating conditions between the “onset-of-nucleate boiling” (wall temperature greater than saturation) and the point of “net vapor generation” is not a parameter that has received considerable focus. In part, this is because there are no thermal or mechanical design or analysis limits that depend on such knowledge. Additionally, it is difficult (perhaps impossible) to directly measure the vapor generation rate in this subcooled region. Two indirect methods have been used to estimate the vapor generation rate under bulk-subcooling boiling conditions: (1) the heat transfer coefficient and (2) the void fraction.

Models and correlations for the heat transfer processes in the subcooled boiling region will often have a convection and a nucleate boiling term. These terms are present because they represent the endpoints of the processes that the model designer deems should be connected through the subcooled boiling region. The two contributions to the heat transfer coefficient model are weighted by enhancement and suppression factors, respectively. However, the weighting functions are usually obtained from experimental data for which the components to the total heat transfer coefficient have not been determined individually. Thus, there is no specific information to individually validate the components. Assigning the vapor generation rate to the boiling component can not be justified.

Various void fraction models have been developed and benchmarked to void data downstream of the point of net vapor generation where an "observable" void fraction exists. Most of these models include a generation term and a condensation term; the net of these contributions is the vapor source term for void fraction. Note that the generation and condensation terms are not benchmarked separately. Hence, the benchmarking only validates the net of the two terms. Additionally, since these models have been developed for void fraction downstream of the location of the net vapor generation, they may not be applicable to the region upstream of net vapor generation, which is of interest in PWRs relative to deposition problems.

Impact of Deposits on Heat Transfer and Fluid Flow. The impact of deposits on heat transfer and fluid flow depends on the specific morphology of the deposits. Generally, deposits in a rod bundle subchannel will tend to divert flow to the subchannels with no, or fewer, deposits. Also, deposits will cause nucleation to begin earlier (at a smaller wall superheat) and the rate of vapor generation to increase over that for a clean surface. The affect of these general characteristics is to increase the rate of both solubility and vaporization driven deposition processes.

A nuclear fuel assembly undergoing continuing deposition may, at some point, impact the fluid flow and/or heat transfer characteristics to the extent that degradation or failure of the fuel rod cladding occur. The cladding failures in the TMI-1 Cycle 10 core [1.3] are believed to have been caused in this fashion.

Deposition Models and Correlations. Deposition models of the different chemical species which may be of importance in modern PWRs will not be discussed herein. It will be assumed that the processes depend on the deposition of particles, dissolution of species, or concentration and deposition of species due to vapor generation. In this context, the focus of this report is on the thermal-hydraulic parameters which may be the key inputs to the chemical processes.

Summary

The following summarizes the fundamental questions in each of the above posed areas:

- Subcooled Forced Convection and the Superheat Threshold for Subcooled Boiling

  Is there a solid experimental basis for the subcooled forced convection heat transfer coefficient at PWR operating conditions in an open lattice rod bundle geometry? The significance of this question pertains to solubility-driven deposition as well as to the threshold of vapor-generation deposition.

  Note that the same fundamental question may be posed regarding the superheat threshold for subcooled boiling. However, the magnitude of the superheat threshold is quite small relative to the forced convection film temperature difference for PWR operating conditions. The uncertainty in the determination of the forced convection heat transfer coefficient is typically much larger than the superheat threshold. Therefore, the focus herein will be the forced convection heat transfer coefficient.

- Impact of Chemicals on the Heat Transfer Coefficient

  Is there a body of knowledge that quantifies the impact of typical PWR chemical additives on the heat transfer? The significance of this question pertains to solubility-driven depositions as well as the threshold of deposition due to vapor generation. In addition, understanding the magnitude of the impact of chemicals may provide clues to unexpected variations in behavior that has been observed in operating PWRs.

- Vapor Generation Rate

  Can existing correlations be used to determine the vapor generation rate for bulk subcooled fluid flows in PWR cores at operating conditions? The question here is how much of the fuel rod cladding surface can be viewed as being cooled by convection vs. nucleation in a subcooled environment at typical PWR design conditions. The second part of the question is, do any of the existing models have a physical basis for dividing the convection and nucleation portion of the heat flux?

- Impact of Deposits on Heat Transfer and Fluid Flow

  This subject will be left for a different report. The focus here will be the status of the technology that influences the initial formation of deposits.

References

1.1. Rootcause Investigation of Axial Power Offset Anomaly, EPRI TR-108320, June 1997.

1.2. Thermal-Hydraulic Bases for Fuel Cycle Designs to Prevent Axial Offset Anomalies, EPRI TR-108781, December 1997.

1.3. TMI-1 Cycle 10 Fuel Rod Failures, Volume 1: Root Cause Failure Evaluations, EPRI TR-108784-V1, October 1998.

1.4. J. Weisman, Letters to the Editors, Nuclear Science and Engineering, Volume 6, Number 1, July 1959.

1.5. D. A. Dingee, W. B. Bell, J. W. Chastain, and S. L. Fawcett, “Heat Transfer from Parallel Rods in Axial Flow,” Battelle Memorial Institute Report BMI-1026, 1955.

1.6. F. W. Staub, G. E. Walmet, R. O. Neimi, “Heat Transfer and Hydraulics, The Effects of Subcooled Voids,” U.S. Atomic Energy Commission Contract AT(30-1)-3679, NYO-3679-8, May 1969.

2
OBJECTIVES

From a thermal design standpoint, there is little need to improve the fidelity of the rod bundle heat transfer model in the subcooled forced convection heat transfer and subcooled boiling regimes. However, the ability to accurately model this region is important because of the sensitivity of deposition processes to the fluid temperature near the wall, the initiation of subcooled vapor generation, and the subcooled vapor generation rate.

The overall objective of this work is to chart the course to the development, verification, and validation of improved thermal-hydraulic information, which will allow the design and operation of fuel cycles with a minimum of economic impact from concerns of developing an adverse axial offset or deposits that may cause fuel failures.

Two tasks are undertaken in this report to assist in addressing the overall objective:

- The first step is to perform a literature review of the state-of-the-art in rod bundle heat transfer at typical PWR operating conditions. This will define what information is available that may answer the fundamental questions in Section 1, Introduction.
- An assessment of the current rod bundle thermal hydraulic information is discussed and recommendations for improving fundamental rod bundle heat transfer knowledge is presented.

3
HEAT TRANSFER FUNDAMENTALS

Introduction

The primary areas of interest for deposition processes in PWRs are the axial locations where (1) the heated surface temperature reaches the saturation temperature, and (2) vapor generation is initiated. The conditions under which these processes occur are first discussed in terms of the standard pool boiling curve, followed by the forced-convection discussion.

The Pool Boiling Curve

The pool boiling curve is generally employed as a convenient reference for discussing the behavior of heated surfaces on which a fluid is boiling. A representation of a pool boiling curve at a fixed pressure is shown in Figure 3-1. The heat flux is shown as a function of the wall superheat, (T_w - T_{sat}), the standard temperature potential for boiling. A brief discussion of the characteristics of the physical processes associated with two-phase heat transfer and the various paths shown in Figure 3-1 is given here.

The characteristics of the boiling curve for pool boiling depend upon the type of energy exchange processes employed to obtain the data. Both heat-flux-controlled and temperature-controlled surfaces are encountered. In the case of the former, the energy is supplied to the heated surface by a constant source of energy such as electrical heaters. For the latter, a boiling or condensing fluid might supply the energy.

At steady-state operating conditions, a nuclear fuel rod is a heat-flux-controlled surface with a nonuniform distribution of heat flux along the rod. In general, the processes which are encountered as the surface temperature is increased in a temperature-controlled condition correspond to those which are encountered as the fluid moves axially along the surface under heat-flux-controlled conditions. The boiling potential (T_w - T_{sat}) increases as the fluid moves from the inlet to the location of the peak heat flux in the reactor core.

- In general, the path BDEF on Figure 3-1 is obtained by use of temperature-controlled surfaces as the surface temperature is increased.
- For the case of a heat-flux-controlled surface, for both forced convection and free convection, the path ABDD′F is obtained as the heat flux is increased. Point D′ represents the new equilibrium state of the surface at the heat flux value q_{CHF}. The departure from nucleate boiling (DNB), or critical heat flux condition (CHF), is a design limit not encountered during normal steady-state operation.

- Experimental results have shown that the path FD′EE′ may be obtained upon reduction of the heat flux for a portion of a non-uniformly heated surface.
- The transition boiling region, path EC of Figure 3-1, for forced convection has been obtained by use of a transient technique which produces a quenching curve for a portion of the test section. This curve follows the path FECE′ of Figure 3-1. The heat flux at point C is less than the initial heat flux at point D. The transition boiling process is not of interest at steady-state operating conditions.
- Some experimental information is available which indicates that the minimum heat flux, point E of Figure 3-1, has different values for steady-state and transient conditions. That is, under transient quench tests, the wall superheat at which the minimum heat flux is attained is higher than the value under steady-state conditions. The condition of the surface of the heated element affects the transient results.

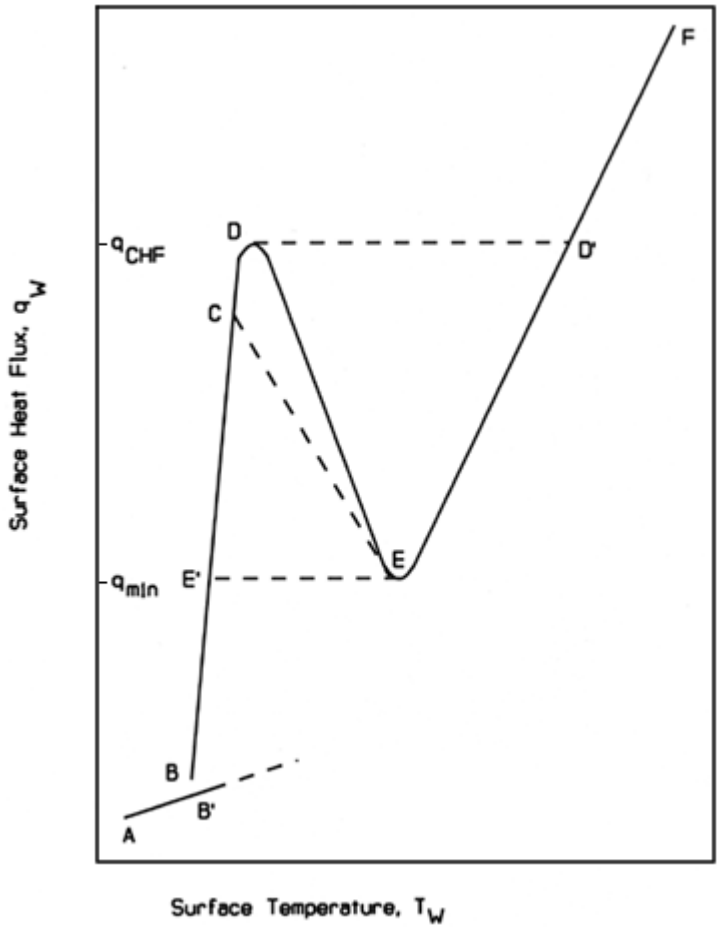

Figure 3-1
Pool Boiling Curve at a Fixed Pressure (Log-Log Plot)

The curve shown in Figure 3-1 is for a fixed pressure. A family of boiling curves is obtained as the pressure is changed. For a given fluid, the heat transfer coefficient correlations that give the surface temperature are functions of the saturation state and transport properties of the fluid.

Forced Convection Heat Transfer Regimes

For the case of forced convection, the “boiling curve” at a given pressure is in fact a family of curves with the mass flux as a primary parameter and the thermodynamic quality as a secondary parameter for each value of the mass flux. The pressure is also a parameter, and for forced convection a boiling surface is usually constructed in place of a boiling curve.

The two-phase flow and heat transfer regimes which may occur in reactor cores are shown in Figure 3-2. The heat transfer regimes shown in Figure 3-2a generally correspond to those encountered in boiling water reactors (BWRs) and those in Figure 3-2b correspond to pressurized water reactors (PWRs). A brief description of these regimes is given here and the relationships to Figure 3-1 are indicated.

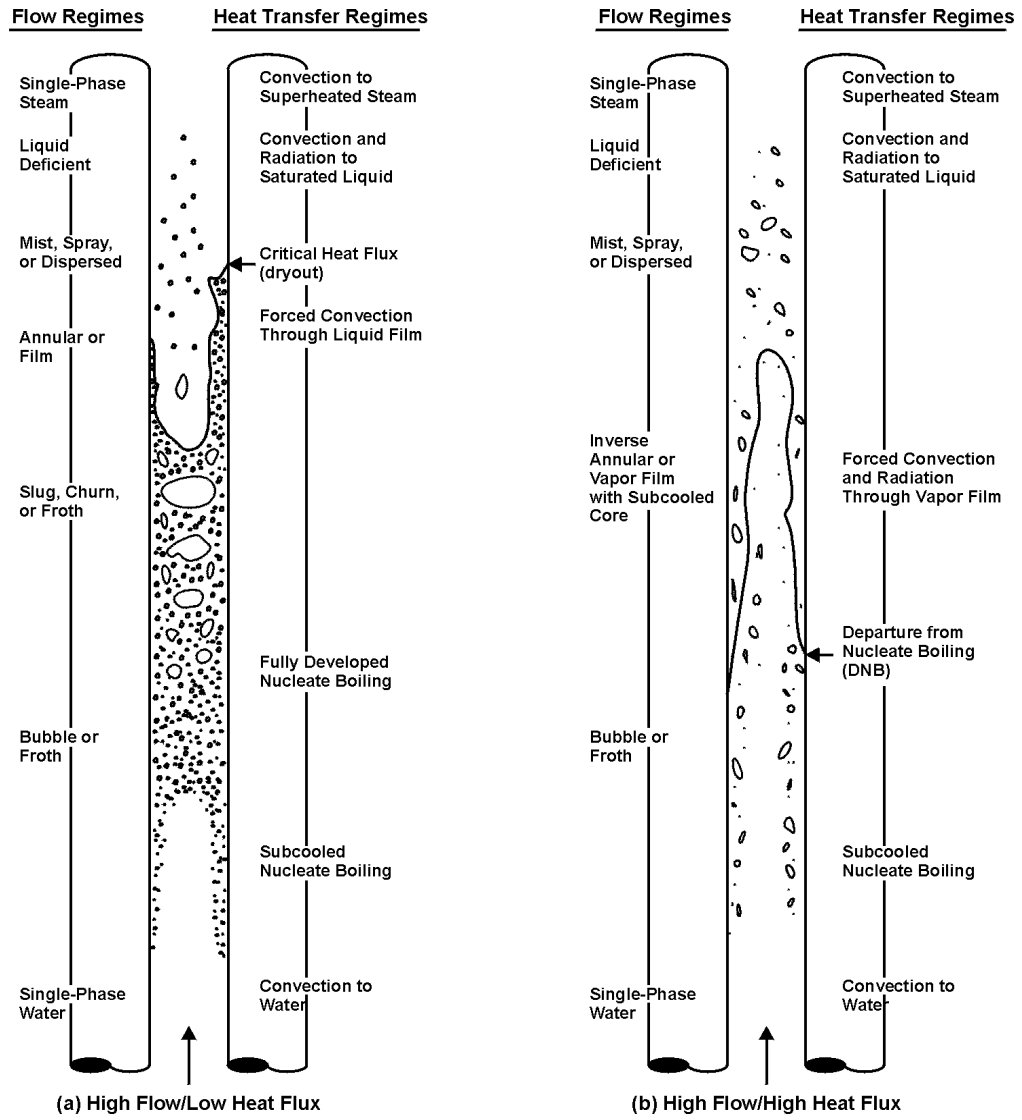

Figure 3-2
Boiling Heat Transfer Regimes in Rod Arrays

At the inlet of the flow channels shown in Figure 3-2, forced convection to single-phase liquid occurs. For the case of relatively high flow rates, the heat transfer coefficient for this regime is fairly well known for flow in simple geometries such as round tubes and annuli. However, for the rod-array geometry of interest the proceeding statement is not true. The literature review in Section 4 shows that there is little credible data for a single-phase, forced-convection heat transfer coefficient correlation applicable to rod arrays. The single-phase liquid convection region corresponds to the path AB of Figure 3-1.

The subcooled boiling regimes shown in Figure 3-2 occur when the flow-channel-average bulk fluid temperature is less than the saturation temperature. Subcooled boiling is initiated at point B and occurs along the path BCD of Figure 3-1.

Onset of Nucleation (ONB). Although the bulk fluid temperature is less than the saturation temperature, the temperature of the fluid adjacent to the clad surface is at, or above, the local saturation temperature, and boiling may begin. The clad surface and a small quantity of the fluid adjacent to the clad are superheated. Downstream of the location where the clad surface temperature reaches the saturation temperature, the liquid adjacent to the clad begins to superheat. The axial location at which the wall and nearby fluid are superheated to the extent that boiling can begin is the location of onset of nucleation (ONB). Vapor bubbles grow and collapse at the few active nucleation sites near the ONB condition.

The potential for local vapor production at the clad surface exists when the clad temperature is at the saturation temperature and significant superheating is not yet present. Generally, models and correlations for initialization of vapor regions in the microscopic imperfections on the clad surface show that as the pressure approaches the critical pressure, less wall superheat is needed for boiling initialization. Additionally, impurities in the fluid that can reduce the surface tension will also act to reduce the wall superheat needed for vapor production.

The wall superheat required to initiate boiling is in general a function of the micro structure of the clad surface, and the thermo-physical and thermodynamic state properties of the fluid. Most empirical descriptions employed in engineering analyses do not contain an accounting of all these details. In addition, no distinction is made between the partial and fully developed subcooled boiling conditions. Empirical correlations are employed to determine the surface temperature at point B and along the path BCD of Figure 3-1.

The vapor generated in the microscopic cracks and crevices on the clad surface will generally recondense into the subcooled liquid. Some vapor bubbles may slide along the clad surface while the recondensation occurs. Only a few nucleation sites are active at the low values of the wall superheat near the ONB location. It is generally pictured that a very thin microlayer of liquid exists on the clad surface at the nucleation sites and under the vapor bubble growing out into the liquid.

Partial Nucleate Boiling. Until the bulk fluid temperature reaches the saturation temperature, the potential exists for vapor generated in the fluid adjacent to the wall to recondense in the fluid which is at a temperature less than the saturation temperature.

Fully-Developed Nucleate Boiling. The nucleate boiling regime occurs as the bulk fluid temperature reaches the local saturation temperature. Almost all the energy addition to the fluid from the fuel rod goes to vapor production, and the heated clad surface will be immersed in a vigorously boiling liquid with many nucleation sites active on the clad surface. For some flow rates and rod-fluid energy exchange rates, the fluid may not attain the saturation state before the CHF point is reached. This latter condition occurs at higher heat flux as shown in Figure 3-2 for PWRs. The fully developed nucleate boiling regime occurs along path B-D of Figure 3-1, depending upon the bulk fluid temperature.

The fully developed nucleate boiling regime may be encountered in PWRs at steady-state operating conditions only in the hottest subchannels.

Other Boiling Heat Transfer Regimes. The remainder of the boiling curve and two-phase boiling heat transfer regimes shown in Figures 3-1and 3-2 are not expected to be encountered in PWRs at steady-state operating conditions and will not be discussed here.

4
REVIEW OF ROD BUNDLE HYDRODYNAMICS AND HEAT TRANSFER REFERENCES

Introduction

In the following discussions specific individual references containing information about rod bundle hydrodynamics and heat transfer are summarized. Some important results of the reviews include:

- The data on which the major correlation for the single-phase liquid heat transfer coefficient in rod bundles is based are significantly deficient relative to the bundle length, other geometric parameters, fluid conditions, and operating states.
- There are no heat transfer data in the open literature, either single-phase or boiling, available for the rod array geometry at typical PWR fluid conditions and chemical species.
- Application of standard engineering models of turbulent flow fields to the rod array geometry is not justified (not fundamentally sound).
- No systematic experimental investigations of heat transfer in rod arrays at PWR steady state operating conditions have been reported in the open literature in about four decades.

The literature reviews are organized in the following categories:

1. Historical reports and papers on which current heat transfer correlations are based.
2. Experimental investigations into rod-array turbulence, friction, and heat transfer.
3. Other references of general interest.

Historical Reports and Papers

Brief summaries of the most important papers addressing single-phase water heat transfer in rod bundles are given in the following paragraphs.

D. A. Dingee, W. B. Bell, J. W. Chastain, and S. L. Fawcett, "Heat Transfer from Parallel Rods in Axial Flow," Battelle Memorial Institute Report BMI-1026, 1955.

D. A. Dingee and J. W. Chastain, "Heat Transfer from Parallel Rods in Axial Flow," Reactor Heat Transfer Conference of 1956, New York, Book 1, p.462.

Dingee and Chastain experimentally examined the convective heat transfer and friction factors using a 3x3 array of 0.5 inch (12.7 mm) outside diameter tubes 23.75 inches (0.603 m) long in both square and triangular pitch arrangements. Pitch-to-diameter (P/D) ratios of 1.12, 1.2, and 1.27 were tested. The experiments were conducted with water as the working fluid with a Prandtl number of 1.18 and 1.75 at the inlet, over a range of Reynolds numbers from 30,000 to 700,000. The Prandtl number will decrease as the water is heated in the test section. The authors concluded that fully-developed hydrodynamic conditions were established at about 12 equivalent wetted diameters downstream from the inlet. (See comments that follow)

Dingee presents an analysis of the constituent errors and concludes that the combination of errors would result in an uncertainty of the heat transfer coefficient of approximately 8 percent. (See comments that follow)

The authors examine peripheral variations in the Nusselt number around an instrumented rod but conclude that while there appear to be significant variations, they do not find any consistent periodic behavior. The variations are concluded to be on the order of the experimental accuracy. This conclusion is supported by a special test that placed the instrumented rod into a concentric tube which preserved the flow area for 1.2 P/D ratio array.

The authors conclude that the experimental Nusselt numbers are approximately 20 percent higher than that predicted by round-tube correlations using the equivalent diameter concept. This is in general agreement with other investigations to be discussed below.

Comments. Because this work forms a substantial part of the basis for the widely used Weisman model (discussed later) for the Colburn coefficient for rod bundles, a detailed analysis of the test has been performed. Appendix A presents an analysis of the test using the EPRI program CORETRAN. Several key conclusions can be drawn from the analysis:

- There is substantial bulk flow redistribution occurring throughout the entire length of the 23.75 inch (0.603 m) test section. Measurements were taken at 6, 12, and 18 inches (0.1524, 0.3048, and 0.4572 m). Since cross flow will impact the turbulence and thus the heat transfer coefficient, it is impossible to draw a conclusion about the heat transfer behavior of the rod bundle geometry relative to a tube. In essence, there can be no fully developed thermal boundary layer until the channel flow distribution has come to its steady state.
- The analysis in Appendix A compares the Dingee experimental Nusselt number results to the Dittus Boelter model where the model results use the CORETRAN predicted local conditions at the instrumented locations. A tube entrance length model is also applied to the data to approximate the entrance effects. Using the tube model should be quite conservative in this situation. The results show substantial scatter and only remote trends. In the *Handbook of Single-Phase Convective Heat Transfer* [4.35], Rehme presents several references that suggest entrance lengths for rod arrays ranging from 30 to 290 L/D.
- The higher Reynolds number data points will have a larger measurement error because the film temperature difference is small relative to the errors in measuring the fluid and inside wall temperature. With a constant power, the wall to bulk temperature difference at the low

Reynolds numbers is on the order of 31.25°C (50°F) where at the high Reynolds numbers the difference is 4.4 to 6.2°C (7 to 10°F). The quoted accuracy of 8% may be suspect at higher Reynolds numbers.

These data and that discussed next represent the only data for subcooled water within the range of Prandtl and Reynolds number of interest for the PWR applications.

P. Miller, J. J. Byrnes, and D. M. Benforado, "Heat Transfer to Water Flowing Parallel to a Rod Bundle," AIChE Journal, Vol. 2, pp. 226, 1956.

These authors conducted one of the earliest experimental investigations of rod bundle heat transfer. A large array of 37 rods arranged in triangular pattern was used for the tests. The measurements were made along a 4-inch (0.1016 m) section at the midsection of one rod. The working fluid was water, the Prandtl number ranged from 1.10 to 2.75, and the Reynolds number from 70,000 to 700,000.

The experimental data showed that the frictional pressure loss was about 60 percent larger than predicted by the usual engineering correlation

$$f_w = 0.046\,Re^{-0.20} \qquad \textbf{Eq. 4-1}$$

The heat transfer coefficient was about 40 percent higher than that predicted with the usual correlation for round tubes. As shown in Section 4 above of this report, a larger friction factor implies a larger heat transfer coefficient. The authors give a correlation of the data to be

$$Nu = 0.036 Re^{0.80}\, Pr^{0.333} \qquad \textbf{Eq. 4-2}$$

Comments. These data and that discussed above represent the only data for subcooled water within the range of Prandtl and Reynolds number that is applicable to the analysis of PWR fuel rod arrays at operating conditions.

However, the test configuration has some potential shortcomings:

The instrumented portion of the test section is only 4 inches (0.1016 m). The authors concluded that the 4-inch (0.1016 m) section was adequate by looking at the relative heat transfer coefficient across an 8-inch (0.2032 m) heated section. The authors comment about axial conduction impacting the readings on the thermocouples at the end of the heated section.

The rod array was unheated except for the short heated section of a single rod. The authors looked at two adjacent heated rods and again concluded that the results were the same. The temperature distribution in the fluid will be quite different than if all the neighboring rods are heated.

While the authors seem to have established that these two potential problems are of no significance, the arrangement is so atypical that one must question the quality of the data.

R. G. Dreissler and M. F. Taylor, "Analysis of Axial Turbulent Flow and Heat Transfer Through Banks of Rods or Tubes," Reactor Heat Transfer Conference of 1956, New York, Book 1, p.416.

The Dreissler work is completely analytical. Dreissler assumed that expressions for eddy diffusivity which has been validated in tubes were applicable to the rod bundle channels. Calculations were performed over a wide Prandtl (0.3 to 300) and Reynolds number (20,000 to 900,000) range. Both square and triangular arrays were examined for various pitch to diameter ratios.

The square array predictions were compared to a few data points from Dingee and Chastain. The Stanton number was plotted as a function of Prandtl number for Reynolds numbers of 30,000 and 300,000. The predictions with a pitch-to-diameter (P/D) ratio of 1.1 match the data at P/D of 1.12 and 1.2 reasonably well. However, it is difficult to assess the functional dependency on P/D given that the predictions for a P/D of 2 are also quite close to the data.

Comments. These results might be useful if CFD modeling for single-phase flow and heat transfer could provide insight for deposition problem in PWR rod arrays. The use of eddy diffusivity from round tubes for rod array analysis may require additional investigation. The conclusion, based on the work for the present report, is that the round-tube eddy-diffusivity is not useful for applications to rod arrays.

J. L. Wantland, "Compact Tubular Heat Exchangers," Reactor Heat Transfer Conference of 1956, New York, Book 1, p.525.

Wantland experimentally examined the heat transfer and friction characteristics of square and triangular pitch rod bundle arrays. The tube outside diameter was 3/16 inch (4.7625 mm) for both bundle arrays. The heat transfer tests were conducted using both resistance heating and in a water-to-water configuration.

The square array test comprised 100 tubes approximately 6 feet (1.8288 m) long enclosed in a square plexiglass shell. The tests were conducted in an apparatus at approximately 45 degrees from vertical. The alternate vertical and horizontal wire spacers were used to maintain 0.020 inch (0.508 mm) spacing. In the resistance heating tests the inside temperature of the tubes were measured by 42 thermocouples at three axial locations in 14 tubes. The instrumented tubes were selected to provide information from the wall cells to the interior cells. The instrumented locations were averaged using weighting factors that favored the interior cells.

Figure 6 in the report presents the square array test data. The water-to-water and resistance-heated results appear to cluster close together for the Reynolds number from 2000 to 10,000. At a Reynolds number of approximately 1500 the results show a significant departure. The Prandtl number range was 3 to 6 for the tests. Wantland fitted the square array results with the following expression:

$$Nu = 0.0155 Re^{0.8} Pr^{0.4} \qquad \text{Eq. 4-3}$$

Wantland performed a general analysis of errors and stated that the "heat transfer characteristics are believed to be accurate with 10%."

Comments. The Wantland results are of no value in the development of a heat transfer coefficient for typical PWR rod bundles. The Prandtl and Reynolds number ranges are far from prototypical operating conditions. The rods are roughly half the diameter of PWR rods, the pitch to diameter ratio is 1.10 vs. about 1.3, and the spacers have no similarity to nuclear fuel assembly rod bundles.

Hypothetically, if the fitting of the Wantland data had confirmed other rod bundle experiments, one could draw the conclusion that the parameter ranges don't matter. However, this was not the case. The Nusselt number correlation happens to agree with a correlation for water given by Kays in his heat transfer text.

The correlation of Eq. 4-3 has a numerical coefficient that is smaller than the standard Dittus-Boelter correlation value of 0.023. Thus, these data are consistent with other experimental and analytical results which indicate that for small P/D ratios, the heat transfer coefficient is smaller than the Dittus-Boelter value.

J. H. Parrette and R. E. Grimble, "Average and Local Heat Transfer Coefficients for Parallel Flow Through a Rod Bundle," Westinghouse Atomic Power Division Report WAPD-TM-180, 1957.

These authors tested a 3x3, square-pitch rod array at P/D of 1.14 and 1.20 with air as the working fluid. The maximum Reynolds numbers tested was 160,000. The experimental data show that the heat transfer coefficient is larger than that predicted by the usual round tube correlations. The Parrette and Grimble test data is of little value for two reasons: the working fluid was air, and the measurement technique was based on the use of a mass transfer principle using napthalene. The authors suggested that the mass transfer method does not give accurate average heat transfer coefficients.

J. Weisman, Letters to the Editors, Nuclear Science and Engineering, Volume 6, Number 1, July 1959.

The Weisman correlation suggests that the leading coefficient in the Dittus-Boelter correlation should be larger than the Dittus-Boelter value of 0.023 when modeling rod bundles. Weisman's correlation is based on data for square pitch rod arrays from Dingee and others discussed above. The Weisman modification to the Dittus-Boelter correlation is

$$Nu = C_W \, Re^{0.80} \, Pr^{0.333} \qquad \textbf{Eq. 4-4}$$

where

$$C_W \, 0.042\left(\frac{P}{D}\right) - 0.024 \qquad \textbf{Eq. 4-5}$$

for square-pitch arrays.

Comments. The Weisman correction to the Dittus-Boelter correlation is widely cited in the literature. To a large degree, the Weisman model is based on the Dingee data. The comments above on the Dingee test and the analysis in Appendix A show that this data is potentially quite flawed for the development of this type of correction which is used in subchannels analysis.

W. A. Sutherland and W. M. Kays, "Heat transfer in Parallel Rod Arrays," General Electric Atomic Power Equipment Department Report GEAP-4637, 1965.

These authors conducted both analytical and experimental studies into turbulent flow and heat transfer in parallel rod arrays. Results from the analytical model were compared with experimental data from heated rod arrays having triangular pitch with P/D of 1.15 and 1.25. Air was the working fluid and the Prandtl number was 0.70 and the Reynolds number ranged from 7,000 to 200,000.

The friction factor data generally fall above the values given by the standard engineering correlations

$$f_w = 0.079\,Re^{-0.25} \qquad \textbf{Eq. 4-6}$$

and

$$f_w = 0.046\,Re^{-0.20} \qquad \textbf{Eq. 4-7}$$

The grid-spacer loss coefficient was also determined from the experimental data.

The model of Kays and Leung, discussed below in this section, was used for the heat transfer analysis. The detailed Kays and Leung analytical method was used with the equivalent-annulus approach to calculate the heat transfer coefficient. The heat transfer coefficient results generally show the same trend with the pitch-to-diameter ratio noted in the other data reviewed above. For P/D ratios greater than about 1.15, the data do not show a dependency on this ratio. Additionally, the data generally fall a little above the correlation for air flow in a round tube (not the Dittus-Boelter correlation) for pitch-to-diameter ratio greater than about 1.15. These results are consistent with the friction factor being greater than the standard correlations given above.

The authors note that because of the limited range of the Prandtl number in many of the experimental investigations reviewed above, the Nusselt number can be reduced to a function of the only Reynolds number.

The authors present a very detailed discussion of many of the papers reviewed above in this section. Several fundamental aspects of applying turbulent-flow models developed for round tubes, and other simple geometries with closed boundaries, to the rod-array geometry are also discussed. Generally, the authors discourage this practice.

Comments. The rod array geometry and working fluid for the experimental data do not correspond to the operating conditions of the PWRs. The report contains an excellent summary

of many important considerations relative to friction and heat transfer in the parallel-array geometry.

M. Khattab, A. Mariy, and M. Habib, "Experimental Heat Transfer in Tube Bundle (Part II)," Atomkernenergie-Kerntechnik, Vol. 45, No. 2, pp. 93-97, 1984.

The authors summarized the experimental results discussed above and conducted additional testing for rod-array heat transfer. A collection of the friction factor and heat transfer coefficient correlations suggested by the literature up to the time the paper was written was presented and predictions compared with experimental data.

The experiments focused on the central and corner rods in a 4x4 array with square pitch, rod diameter of 10 mm (0.39 inches), heated length 600 mm (23.6 inches), and P/D ratio of 1.5. Subcooled water was the working fluid and the Reynolds number ranged from 4900 to 14,000 and the Prandtl number from 3.9 to 5.39. The data showed that the heat transfer coefficient for the central rod was about 27 percent larger than for the corner rod. Temperature distributions axially along the central and corner rods are given in the paper.

The authors report that of several existing correlations, the Dittus-Boelter more closely predicted the corner-rod data and that a correlation by Miller more closely predicted the central-rod data.

Heat transfer coefficient correlations, expressed in terms of the Nusselt number, based on the bundle-average flow rate and equivalent wetted diameter, were obtained from the data and found to be

$$Nu = 0.0064 Re^{0.98} Pr^{0.33} \qquad \textbf{Eq. 4-8}$$

for the central rod, and

$$Nu = 0.2182 Re^{0.55} Pr^{0.33} \qquad \textbf{Eq. 4-9}$$

for the corner rod.

Comments. The ranges of geometry and operating conditions for these data make them of little value for PWR applications.

Rod Array Turbulence, Friction, and Heat Transfer

W. M. Kays and E. Y. Leung, "Heat Transfer in Annular Passages - Hydrodynamically Developed Turbulent Flow with Arbitrarily Prescribed Heat Flux," International Journal of Heat and Mass Transfer, Vol. 6, pp. 537-557, 1962.

This paper is not directly related to rod-array heat transfer. However, the detailed analytical methods introduced in the work for turbulent flow have proven to be very fundamental and useful in convective heat transfer modeling and analyses. The results given in the paper are the standard method for calculation of the convective heat transfer coefficient for turbulent flow in

annular flow channels. The method is also used in conjunction with the equivalent-annulus approach for analyses of heat transfer in rod arrays. The equivalent-annulus approach is given in Section 5.

The thermal and hydrodynamic problem is formulated as a two-dimensional plane turbulent shear flow. Empirical turbulent velocity and eddy diffusivity profiles form the basis of the analytical model. The results of the model were validated with experimental data for air flow with a Prandtl number of 0.70. At large outer-to-inner diameter ratios the data and model results show that the conditions for a round tube are obtained. The results are given in a series of tables and graphs and are not repeated here.

The predictions of the model compared with experimental data from uni-and bilaterally heated annuli show very good agreement for both the developing entry and fully developed regions.

The authors also validated the modeling with experimental data for turbulent flows in round tubes. The correlation of the heat transfer experimental data for round tubes was given to be

$$Nu = 0.022\,Re^{0.8}\,Pr^{0.5} \qquad \textbf{Eq. 4-10}$$

Comments. The analytical model given in this paper, and used in the Sutherland and Kays report mentioned above, might prove useful to application to PWR subchannels if the flows in a rod array can be modeled as plane, two-dimensional turbulent shear flows. However, there is no evidence that this is the case.

J. Marek, K. Maubach, and K. Rehme, "Heat Transfer and Pressure Drop Performance of Rod Bundles Arranged in Square Arrays," International Journal of Heat and Mass Transfer, Volume 16, pp. 2215-2228, Pergamon Press 1973.

The objective of the work was to investigate friction and heat transfer in 3x3 and 4x4 rod bundles with square pitch. The Reynolds number range, 10,000 to 30,000, is low relative to what is needed for modeling at PWR operating conditions. Additionally, helium was the working fluid and a single P/D ratio, 1.283, was investigated. At the larger Reynolds numbers covered by the experiments, the data are somewhat useful.

The heat transfer coefficient for the 3x3 rod array was about 7% less and the 4x4 array about 15% less than the Dittus-Boelter value. The authors attribute the differences from the Dittus-Boelter value to the effects of the wall-to-rod gap near the shroud of the array. The 4x4 array had a larger gap than the 3x3 array; more coolant flowed along the gap, the temperature rise for the coolant adjacent to the instrumented rod was higher, the rod-wall temperature was higher, and thus the apparent heat transfer coefficient was lower than would be indicated by the bundle-average temperature rise.

These authors also provide an opinion that the Dingee and Chastain measurements were not accurate. This assessment is based, in part, on the fact that the equivalent-annulus is a very good model for flow in rod arrays with P/D > 1.2. The Dingee and Chastain friction factor and heat transfer coefficient results fall well above the equivalent-annulus lines and thus the present authors conclude that the measurements are not accurate.

Comments. In addition to their own test results, Marek, Maubach, and Rehme summarized six experimental and seven theoretical references. They close the paper with the observation that additional data are needed in order to reach "safe" conclusions about the Nusselt number.

D. S. Rowe, "Measurement of Turbulent Velocity, Intensity and Scale in Rod Bundle Flow Channels," Battelle Pacific Northwest Laboratories Report, BNWL-1736, 1973.

The next report is a summary of the same experimental data and analysis as given in this report.

D. S. Rowe, B. M. Johnson, and J. G. Knudsen, "Implications Concerning Rod Bundle Crossflow Mixing Based on Measurements of Turbulent Flow Structure," International Journal of Heat and Mass Transfer, Vol. 17, pp. 407-419, 1974.

The paper reports on an experimental program performed to investigate the effects of sub-channel geometry on turbulent flows in rod arrays. Water was the working fluid and by varying the water temperature, the Reynolds number ranged from 50,000 to 200,000. The pitch-to-diameter ratio was 1.125 and 1.25. Large-scale rods were used.

The data indicated macroscopic flow processes, including secondary and pulsating flows, adjacent to the rod-to-rod gap. The frequency of the pulsations increased as the rod spacing was decreased. These data were the first to identify these processes and investigation of the macroscopic flows continues to this day.

J. D. Hopper, "Developed Single Phase Turbulent Flow Through a Square-Pitch Rod Cluster," Nuclear Engineering and Design, Vol. 60, pp. 365-379, 1980.

The paper reports the results of an experimental investigation of fully-developed turbulent flow of air in two square-pitched rod arrays with P/D of 1.194 and 1.107. The mean velocity distribution, wall shear stress, and the six elements of the symmetrical Reynolds stress tensor were measured. The departure of the turbulent flow structure from the axisymmetrical round tubes case was a function of P/D. The departure was most noticeable in the gap between the rods.

The data for the mean velocity distribution showed good agreement with the usual engineering law-of-the-wall for both values of the pitch-to-diameter ratio. The mean velocity was given by

$$U^+(r,\theta) = \frac{1}{\kappa}\ln y^+ + C \qquad \textbf{Eq. 4-11}$$

with $\kappa = 0.40$ and C=5.5. The wall friction velocity, used to scale the mean velocity, was based on a friction factor 1.13 times the round tube value as shown by the data. The Reynolds number was about 48,000.

The axial (u'), radial (v'), and azimuthal (w') velocity fluctuations were all found to be larger than the corresponding round tube values for both pitch-to-diameter ratios. The authors note that Rowe, mentioned above, has also reported strong velocity fluctuations, especially in the gap region, for turbulent flow of water in square-pitched rod arrays. Consequently, the radial turbulent shear stress is larger than that in a round tube and thus the friction factor is larger too.

The data indicate the possibility of the existence of a secondary flow structure imposed on the mean flow.

The turbulent kinetic energy, $\frac{1}{2}(u'u'+v'v'+w'w')$ is also larger than the round tube value.

Comments. The experimental results indicate that the usual κ–ε two-parameter turbulence model will not predict these data.

J. D. Hooper and D. H. Wood, "Fully Developed Rod Bundle Flow over a Large Range of Reynolds Number," Nuclear Engineering and Design, Vol. 83, pp. 31-46, 1984.

An experimental investigation of fully developed turbulent flow of air in a rod array with square pitch. Six rods, 9.14 m (360 inches) long, 14 cm (5.5 inches) rod diameter with pitch-to-diameter 1.107, and Reynolds number range of 22,600 to 207,600. The length of the rods provided 128 hydraulic diameters. The primary objective of the work was to investigate the presence of mean secondary flow. Previous investigations had indicated the possibility of secondary flows. The experimental data did not show mean secondary flows.

The experimental data show the departure from round tube turbulence models and data in the gap region between the rods. This departure has been noted above in several references. The radial and azimuthal eddy viscosities were not equal so that the usual assumption of isotropic turbulence is not valid.

Comments. These results again illustrate that application of the usual engineering closure models to the rod array geometry will not be successful.

M. Hudina and M. Huggenberger, "Pressure Drop and Heat Transfer in Gas-Cooled Rod Bundles," Nuclear Engineering and Design, Vol. 97, pp. 347-360, 1986.

This is a specialized investigation that is not of general interest.

K. Rehme, "The Structure of Turbulent Flow Through Rod Bundles," Nuclear Engineering and Design, Vol. 99, pp. 141-154, 1987.

This reference presents experimental results for structure of turbulent flow in a simple test channel consisting of four rods in a straight row. The region from between the rods to the wall are investigated. The axial and azimuthal turbulence intensity is presented and compared to circular tube models. The authors' general conclusion is that turbulent flow through rod bundles greatly differs from turbulent flow through circular tubes

In addition, a large list of references to other investigations on the structure of turbulence is included in the article.

Comments. The results are of limited value for application to PWR open lattice rod arrays because of the close proximity of the walls.

K. Rehme, "Experimental Observations of Turbulent Flow Through Subchannels of Rod Bundles," Experimental Thermal and Fluid Sciences, Vol. 2, pp. 341-349, 1989.

The author gives the results of an experimental investigation into the structure of the turbulence in the wall subchannels of a rod array. The primary objective of the experiment was to get data that might improve the understanding of the departure from round tube turbulence in the rod-gap and wall-gap regions. As noted in several of the references given previously, the departure has been suspected but definitive data have not been available. The authors give a good summary of the various indications from previous experiments.

A single line of four rods bounded by walls formed the array, and air at atmospheric pressure was the working fluid. The rods were 7.0 m (275.6 inches) long. The actual rod diameter is not given, but it is reported that they were from 20 to 25 times larger in diameter than typical fuel rods. The rod diameter was large so that the flow field could be resolved in the rod-gap and wall-gap regions. The pitch-to-diameter ratio was varied from 1.036 to 1.40 and the wall-to-diameter ratio from 1.026 to 1.40. The lower value for these ratios is quite small and thus the need to scale up the rod diameter.

The experimental results clearly showed that the structure of the turbulence in the rod-gap and wall-gap regions of a rod array is significantly different from that in a round tube, especially for smaller pitch-to-diameter and wall-to-diameter ratios (< about 1.2). Computer codes using turbulence models with model parameters adjusted to round tube data will fail to predict rod array flow fields. Anisotropic eddy viscosities or the additional production of kinetic energy must be modeled in order to predict these rod array flows. Additionally, the data indicated the presence of a pulsating flow between the subchannels. This flow contributes to the high turbulent shear stress.

Comments. Experiments conducted by Tapucu and Merilo [4.19, 4.20] have also shown the presence of pressure oscillation between subchannel. The flow channel for these experiments was only two subchannels with an orifice between them. The data of both Rehme and Tapucu and Merilo were obtained in a geometry for which the flow channel provides confinement of the flow. That is, there is no place for the fluid to redistribute in either of the experimental arrangements. The small, confined flow channels may contribute to the pressure pulsations, and these may not be present in large-scale rod arrays.

S. V. Moller, "On Phenomena of Turbulent Flow Through Rod Bundles," Experimental Thermal and Fluid Sciences, Vol. 4, pp. 25-35, 1991.

An experimental investigation into the axial and azimuthal turbulence intensities in the rod-gap region of rod arrays. As the rod-to-rod gap size decreases, these intensities increase and the increase has been associated with the pulsating flow between the subchannels. The primary objective was to obtain additional information about the quasi-periodic fluctuations and how to characterize them for modeling rod-array turbulence.

The author states that the periodic pulsations were first observed by Hofmann and reported in an unpublished report. As noted above in this section, Rowe had also observed the same behavior in

the early 1970s. Rowe's experiments were conducted with water as the working fluid in square-pitched rod bundles with P/D = 1.25 and 1.125.

Moller's experiments were conducted with air as the working fluid in the single-row-of-rods used by Rehme (1989) in the previous paper above. The experimental results indicate that the flow and pressure pulsations are associated with large regular eddies near the rod-gap region. The fluid motion due to the eddies gives rise to both subchannel-to-subchannel mixing and high values of the local heat transfer coefficient.

S. V. Moller, "Single-Phase Turbulent Mixing in Rod Bundles," Experimental Thermal and Fluid Sciences, Vol. 5, pp. 26-33, 1992.

This paper gives the results of additional investigations into the effects of the pulsating motion discussed in the previous paper (Moller 1991). The author presents a mixing-coefficient correlation for use in subchannel and porous-media models of flows in rod arrays.

X. Wu and A. C. Trupp, "Experimental Study on the Unusual Turbulence Intensity Distributions in Rod-to-Wall Gap Regions," Experimental Thermal and Fluid Science, Vol. 6, pp. 360-370, 1993.

This is an experimental investigation into the large turbulence intensities and pulsating flow noted in several papers above. The geometry was a single rod located in a trapezoidal flow channel. The data show the same behavior noted by several investigators listed above.

Comments. However, note that these data, and those listed above, demonstrate that the large turbulence intensities and pulsating flow have been from flow channels with a small number of rods closely confined by walls.

The authors note that accurate prediction of the heat transfer coefficient for turbulent flow in rod arrays will require complete understanding of the turbulent flow field structure in the array.

L. Meyer, "Measurements of Turbulent Velocity and Temperature in a Central Channel of a Heated Rod Bundle," Nuclear Engineering and Design, Vol. 146, pp. 71-82, 1994.

In contrast to all the papers listed above, this experimental investigation looked at heated flows in a rod array. The focus of the work was for the gas-cooled reactor designs so that the rods were arranged in triangular pitch, the P/D was 1.12, the shroud was hexagonal, and the working fluid was a gas. Additionally, the array was tested in a horizontal position. The total length of the working section was 11.50 m (453 inches) with an unheated entrance of 4.60 m (181 inches) and a heated length of 6.90 m (272 inches). The L/D_{hy} for the heated length was 128.

Comments. The results of the experiments indicate that there is less difference between the turbulence for a central subchannel in the heated array and the round tube case than for a wall-subchannel in the isothermal case. All the previous investigations were for isothermal flow.

L. Meyer and K. Rehme, "Large Scale Turbulence Phenomena in Compound Rectangular Channels," Experimental Thermal and Fluid Sciences, Vol. 8, pp. 286-304, 1994.

The authors report on an experimental investigation into the pulsating-flow phenomena noted previously in several reports. A number of geometries were tested to complement the single-row-of-rods and rod-in-trapezoid cases mentioned above. All the geometries tested were of the same general characteristic of two confined flow channels coupled by a small flow area.

Comments. The authors conclude that the pulsating-flow phenomena will be present whenever two large flow areas are coupled by a small flow area. Thus, it may be present in rod arrays as the subchannels are coupled by the small rod-gap region.

T. Krass and L. Meyer, "Characteristics of Turbulent Velocity and Temperature in a Wall Channel of a Heated Rod Bundle," Experimental Thermal and Fluid Sciences, Vol. 12, pp. 75-86, 1996.

This is a continuation of the experimental work of (Meyer, 1994) with P/D ratio of 1.12 and wall-gap-to-diameter ratio of 1.06. The focus on this work is the wall channels in contrast to the previous work of Meyer.

The experimental data show the large-scale periodic fluctuations in velocity and temperature that have been measured in isothermal test sections. These fluctuations are the main source of inter-subchannel mixing and transport of heat and momentum.

Kye Bock Lee and Ho Cheol Jang, "A Numerical Prediction on the Turbulent Flow in Closely Spaced Bare Rod Arrays by a Nonlinear k-e Model," Nuclear Engineering and Design, Vol. 172, pp. 351-357, 1997.

These authors show that, in agreement with experimental data, the usual k-e two-equation turbulence model will not predict the turbulence in the rod-gap region of a rod array. The difference between measurements and experimental data will increase as the P/D ratio decreases.

T. Krass and L. Meyer, "Experimental Investigation of Turbulent Transport of Momentum and Energy in a Heated Rod Bundle," Nuclear Engineering and Design, Vol. 180, pp. 185-206, 1998.

This is a continuation of the work of (Meyer, 1994) with the P/D ratio reduced to 1.06 from 1.12 as used by Meyer. The results of measurements made in a central subchannel show the following. The highest clad surface temperature is reached directly in the gap between the rods. Near the center of the subchannel, farthest away from a wall, the turbulence structure is similar to that in a round tube. In the rod-gap region the turbulence deviates from the round tube structure and the deviation increases as the P/D ratio decreases. The anisotropy of the heat and momentum transfer are comparable and increases as the P/D ratio decreases.

Sin Kim and Goon Cherl Park, "Analysis of Turbulent Mixing in Rod Bundles with an Anisotropic Turbulent Diffusion Model Based on the Flow Pulsation Phenomenon," Nuclear Technology, Vol. 122, pp. 284-294, 1998.

The authors have incorporated the anisotropic eddy diffusivity and pulsating secondary flow effects into a turbulence model for applications to rod arrays with a CFD code. They show that models based on the isotropic-turbulence assumption do not predict the turbulent flow field.

General Interest Studies

M. J. Gruszcynski and R. Viskanta, "Heat Transfer to Water from a Vertical Tube Bundle under Natural Circulation Conditions," Argonne National Laboratory report, ANL-83-7, 1983.

K. P. Hallinan and R. Viskanta, "Heat Transfer from a Vertical Tube Bundle under Natural Circulation Conditions," International Journal of Heat and Fluid Flow, Vol. 6, No. 4, pp. 256-264, 1985.

These two papers deal mainly with flows that are in the natural circulation or mixed-convection regimes and are thus of little use for the understanding PWR operating conditions.

M. Hudina and M. Huggenberger, "Pressure Drop and Heat Transfer in Gas-Cooled Rod Bundles," Nuclear Engineering and Design, Vol. 97, pp. 347-360, 1986.

The objective of these tests was to determine the pressure drop and heat transfer characteristics of rods with roughened surfaces. The experiments were conducted with carbon dioxide at high pressure and flow rate.

One observation that is applicable to the design of future experiments conducted in larger arrays, up to 37 rods in a hexagonal bundle, indicated that a rod must be located at least three rows away from the shroud in order to respond as a rod in an infinite array.

Comments. Other than the single observation given just above, the data are not in any way applicable to the analysis of PWR rod bundle thermal-hydraulics.

A. K. Mohanty and K. M. Sahoo, "Turbulent Flow and Heat Transfer in Rod-Bundle Subchannels," Nuclear Engineering and Design, Vol. 106, pp. 327-344, 1988.

The objective of this analytical work was to investigate the applicability of several turbulence closure models to calculation of detailed thermal-hydraulic distributions with the subchannels of rod arrays. The calculations were done with the molecular Prandtl number of 0.70, corresponding to gases. Algebraic and differential turbulence closure models were investigated. The turbulence modeling based on models for flows in annuli is considered to be more applicable to rod-arrays than round-tube closure models. The rod pitch-to-diameter ratio varied from 1.10 to 1.50 and the Reynolds number from 20,000 to 150,000.

The calculated results for the Nusselt number were about 20 to 25% larger than those estimated by the Weisman correlation which are in turn about 10% larger than the standard Dittus-Boelter correlation.

For the single Prandtl number the authors give the correlations from the calculated results to be

$Nu = 0.0053Re^{0.93}$

for square-pitch array, and

$Nu = 0.0061Re^{0.93}$

for triangular-pitch arrays.

The Blasius correlation for the friction factor

$f_w = 0.079Re^{-0.25}$

underpredicted the calculated friction factor.

Comments. This paper may be useful if CFD analysis is deemed to provide useful information for understanding deposition processes in PWR rod arrays. The analytical results compared to the Weisman correlation are interesting because they are so much larger than those predicted by the correlation. The Reynolds number dependency in the correlations given above is way out of line with all other results we have seen. Additionally, many of the papers reviewed previously indicate that the usual engineering models for turbulence are not applicable to the rod-array geometry.

It is not of general interest and has no direct application to the PWR rod array analysis.

Sung-Ho Kim and Mohamed S. El-Genk, "Heat Transfer Experiments for Low Flow of Water in Rod Bundles," International Journal of Heat and Mass Transfer, Vol. 32, pp. 1321-1336, 1989.

The objective of the work was to determine the effects of gravity on the friction and heat transfer characteristics for rod bundles. The Reynolds number covered the range from about 80 to about 50,000 and the Prandtl number, with water as the working fluid, ranged from 3 to 8.5. These parameters are outside the range of interest for operating PWR reactors.

The rod arrays were made of seven rods arranged in triangular pitch and contained in a hexagonal shroud. Three rod pitch-to-diameter ratios, 1.25, 1.38, and 1.50 were tested. The rod diameter was 0.0127 m (0.5 inch), and the heated length of the rods was 0.9044 m (35.6 inches) with an unheated inlet section 0.513 m (20.2 inches) long to provide for fully-developed hydrodynamic conditions.

For the larger Reynolds number ranges, the Weisman modification to the Dittus-Boelter correlation accurately predicted the bundle-average heat transfer data for P/D = 1.38 and 1.5 for the smaller P/D = 1.25, the Weisman correlation slightly underpredicted the data.

Comments. These data, while for water flowing in an array, are not typical of operating conditions for PWR cores. The Prandtl number is too large, the pitch is triangular, and the Reynolds number range is too small. It is interesting that, on a bundle-average basis, the data validate the Weisman correction to the Dittus-Boelter correlation.

A. K. Mohanty, S. C. Haldar and S. Sengupta, "Low Reynolds Number Flow and Heat Transfer Experiments in 7-Rod Vertical Bundles," Nuclear Engineering and Design, Vol. 143, pp. 83-93, 1993.

The objective of the work was to investigate the effects of gravity through buoyancy on friction and heat transfer in rod bundles. Thus, the Reynolds number range is quite low relative to what is needed for modeling at PWR operating conditions. Additionally, air was the working fluid. At the larger Reynolds numbers covered by the experiments, buoyancy effects are small and the data are somewhat useful.

The experimental bundles were seven-rod arrays arranged in a circle with one central rod surrounded by six rods. The rod diameter was 0.012 m (0.472 inch), the P/D ratio was 2.71, the length was 1.20 m (47.2 inches), and the inside diameter of the shroud was 0.0545 m (21.5 inches). For such small arrays, wall effects due to the shroud cannot be neglected and the shroud-to-rod-diameter ratio was 4.54. The experimental data show significant heat transfer differences between the central and peripheral rods.

The Reynolds number was varied from about 900 to about 30,000. A transition from laminar to turbulent flow regimes was not evident in the data and at the larger Reynolds number the bundle-average friction factor could be represented by the standard empirical correlation

$$f_w = 0.046 Re^{-0.20}$$

where Reynolds number is based on the bundle wetted equivalent diameter.

Bundle-average pressure drop and friction data were obtained, and to relate the heat transfer characteristics to the friction properties through the Reynolds analogy, the rod array was modeled as a porous media. The porosity of the array, and the wetted and heated specific surface area density, can be related to the P/D ratio and the geometric details of the shroud and array. The modeling approach was very successful with the data clearly showing the applicability of the Reynolds analogy.

The bundle-average heat transfer coefficient, using the Reynolds analogy was

$$Nu = 0.24 Ref_w$$

Comments. While the Reynolds analogy, and other heat and momentum analogies, are very useful in general, they cannot be applied to the open lattice PWR rod arrays unless subchannel-

level pressure drop data are available. Generally, only bundle-average pressure drop data are obtained from rod-array experiments.

References

4.1. D. A. Dingee, W. B. Bell, J. W. Chastain, and S. L. Fawcett, "Heat Transfer from Parallel Rods in Axial Flow," Battelle Memorial Institute Report BMI-1026, 1955.

4.2. D. A. Dingee and J. W. Chastain, "Heat Transfer from Parallel Rods in Axial Flow," Presented at the Reactor Heat Transfer Conference of 1956, New York, United States Atomic Energy Commission Report, TID-7529, Book 1, pp. 462-501, 1957.

4.3. P. Miller, J. J. Byrnes, and D. M. Benforado, "Heat Transfer to Water Flowing Parallel to a Rod Bundle," AIChE Journal, Vol. 2, pp. 226, 1956.

4.4. Robert G. Deissler and Maynard F. Taylor, "Analysis of Axial Turbulent Flow and Heat Transfer Through Banks of Rods or Tubes," Presented at the Reactor Heat transfer Conference of 1956, New York, United States Atomic Energy Commission Report, TID-7529, Book 1, pp. 416-461, 1957.

4.5. J. L. Wantland, "Compact Tubular Heat Exchangers," Presented at the Reactor Heat transfer Conference of 1956, New York, United States Atomic Energy Commission Report, TID-7529, Book 1, pp. 525-548, 1957.

4.6. J. H. Parrette and R. E. Grimble, "Average and Local Heat Transfer Coefficients for Parallel Flow Through a Rod Bundle," Westinghouse Atomic Power Division Report WAPD-TM-180, 1957.

4.7. Joel Weisman, "Heat Transfer to Water Flowing Parallel to Tube Bundles," Nuclear Science and Engineering, Vol. 6, No. 1, pp. 78-79, 1959.

4.8. W. A. Sutherland and W. M. Kays, "Heat Transfer in Parallel Rod Arrays," General Electric Atomic Power Equipment Department Report GEAP-4637, 1965.

4.9. M. Khattab, A. Mariy, and M. Habib, "Experimental Heat Transfer in Tube Bundle (Part II)," Atomkernenergie-Kerntechnik, Vol. 45, No. 2, pp. 93-97, 1984.

4.10. W. M. Kays and E. Y. Leung, "Heat Transfer in Annular Passages - Hydrodynamically Developed Turbulent Flow with Arbitrarily Prescribed Heat Flux," International Journal of Heat and Mass Transfer, Vol. 6, pp. 537-557, 1962.

4.11. J. Marek, K. Maubach, and K. Rehme, "Heat Transfer and Pressure Drop Performance of Rod Bundles Arranged in Square Arrays," International Journal of Heat and Mass Transfer, Vol. 16, pp. 2215-2228, 1973.

4.12. D. S. Rowe, "Measurement of Turbulent Velocity, Intensity and Scale in Rod Bundle Flow Channels," Battelle Pacific Northwest Laboratories Report, BNWL-1736, 1973.

4.13. D. S. Rowe, B. M. Johnson, and J. G. Knudsen, "Implications Concerning Rod Bundle Crossflow Mixing Based on Measurements of Turbulent Flow Structure," International Journal of Heat and Mass Transfer, Vol. 17, pp. 407-419, 1974.

4.14. J. D. Hooper, "Developed Single Phase Turbulent Flow Through a Square-Pitch Rod Cluster," Nuclear Engineering and Design, Vol. 60, pp. 365-379, 1980.

4.15. J. D. Hooper and D. H. Wood, "Fully Developed Rod Bundle Flow Over a Large Range of Reynolds Number," Nuclear Engineering and Design, Vol. 83, pp. 31-46, 1984.

4.16. M. Hudina and M. Huggenberger, "Pressure Drop and Heat Transfer in Gas-Cooled Rod Bundles," Nuclear Engineering and Design, Vol. 97, pp. 347-360, 1986.

4.17. K. Rehme, "The Structure of Turbulent Flow Through Rod Bundles," Nuclear Engineering and Design, Vol. 99, pp. 141-154, 1987.

4.18. K. Rehme, "Experimental Observations of Turbulent Flow Through Subchannels of Rod Bundles," Experimental Thermal and Fluid Sciences, Vol. 2, pp. 341-349, 1989.

4.19. A. Tapucu, "Studies on Diversion Cross-Flow between Two Parallel Channels Communicating by a Lateral Slot. I: Transverse Flow Resistance Coefficient," Nuclear Engineering and Design, Vol. 42, pp. 297-306, 1977.

4.20. A. Tapucu and M. Merilo, "Studies on Diversion Cross-Flow between Two Parallel Channels Communicating by a Lateral Slot. II: Axial Pressure Variations," Nuclear Engineering and Design, Vol. 42, pp. 307-318, 1977.

4.21. S. V. Moller, "On Phenomena of Turbulent Flow Through Rod Bundles," Experimental Thermal and Fluid Sciences, Vol. 4, pp. 25-35, 1991.

4.22. S. V. Moller, "Single-Phase Turbulent Mixing in Rod Bundles," Experimental Thermal and Fluid Sciences, Vol. 5, pp. 26-33, 1992.

4.23. X. Wu and A. C. Trupp, "Experimental Study on the Unusual Turbulence Intensity Distributions in Rod-to-Wall Gap Regions," Experimental Thermal and Fluid Science, Vol. 6, pp. 360-370, 1993.

4.24. L. Meyer, "Measurements of Turbulent Velocity and Temperature in a Central Channel of a Heated Rod Bundle," Nuclear Engineering and Design, Vol. 146, pp. 71-82, 1994.

4.25. L. Meyer and K. Rehme, "Large Scale Turbulence Phenomena in Compound Rectangular Channels," Experimental Thermal and Fluid Sciences, Vol. 8, pp. 286-304, 1994.

4.26. T. Krass and L. Meyer, "Characteristics of Turbulent Velocity and Temperature in a Wall Channel of a Heated Rod Bundle," Experimental Thermal and Fluid Sciences, Vol. 12, pp. 75-86, 1996.

4.27. Kye Bock Lee and Ho Cheol Jang, "A Numerical Prediction on the Turbulent Flow in Closely Spaced Bare Rod Arrays by a Nonlinear k-e Model," Nuclear Engineering and Design, Vol. 172, pp. 351-357, 1997.

4.28. T. Krass and L. Meyer, "Experimental Investigation of Turbulent Transport of Momentum and Energy in a Heated Rod Bundle," Nuclear Engineering and Design, Vol. 180, pp. 185-206, 1998.

4.29. Sin Kim and Goon Cherl Park, "Analysis of Turbulent Mixing in Rod Bundles with an Anisotropic Turbulent Diffusion Model Based on the Flow Pulsation Phenomenon," Nuclear Technology, Vol. 122, pp. 284-294, 1998.

4.30. M. J. Gruszcynski and R. Viskanta, "Heat Transfer to Water from a Vertical Tube Bundle under Natural Circulation Conditions," Argonne National Laboratory report, ANL-83-7, 1983.

4.31. K. P. Hallinan and R. Viskanta, "Heat Transfer from a Vertical Tube Bundle under Natural Circulation Conditions," International Journal of Heat and Fluid Flow, Vol. 6, No. 4, pp. 256-264, 1985.

4.32. A.K. Mohanty and K. M. Sahoo, "Turbulent Flow and Heat Transfer in Rod-Bundle Subchannels," Nuclear Engineering and Design, Vol. 106, pp. 327-344, 1988.

4.33. Sung-Ho Kim and Mohamed S. El-Genk, "Heat Transfer Experiments for Low Flow of Water in Rod Bundles," International Journal of Heat and Mass Transfer, Vol. 32, pp. 1321-1336, 1989.

4.34. A. K. Mohanty, S. C. Haldar and S. Sengupta, "Low Reynolds Number Flow and Heat Transfer Experiments in 7-Rod Vertical Bundles," Nuclear Engineering and Design, Vol. 143, pp. 83-93, 1993.

4.35. S. Kakac, R. K. Shah, W. Aung, "Handbook of Single-Phase Convective Heat Transfer," John Wiley & Sons, 1987.

5
HEAT TRANSFER MODELS AND CORRELATIONS

Introduction

Some of the models and correlations typically used to calculate the heat transfer coefficient, and thus the clad-wall temperature, for both single-phase forced convection heating and subcooled boiling are reviewed in this section. The basis of the models and correlations, either theoretical or empirical, will also be given. The models which have a more firm theoretical basis may prove to be applicable to wider ranges of geometry and operating states than those which are primarily based on empirical fitting of experimental data. Additionally, a model having a firm theoretical foundation may provide an improved functional form for use in development of new correlations of experimental data for rod bundle heat transfer coefficients.

Heating Single-Phase Liquid

The coolant entering the core of a PWR at steady-state operating conditions is a subcooled single-phase liquid. The liquid is heated by convective heat transfer between the coolant and the fuel-clad surface and by direct moderator heating. The axial location along the fuel at which the clad surface temperature reaches the saturation temperature marks the beginning of subcooled boiling on the surface of the clad. That location is determined by the distribution of the power along the fuel rod, the mass flow rate of the coolant and its inlet temperature, and the heat transfer coefficient between the clad and the coolant.

Nomenclature

The basic quantities of interest include the bulk-average fluid temperature, the wall temperature, and the saturation temperature at the local pressure. The bulk-average fluid temperature will be denoted T_f, the wall temperature T_w, and the saturation temperature T_{SAT}.

The subcooling of the liquid phase below the saturation temperature is denoted

$$\Delta T_{fSUB} = T_{SAT} - T_f$$

The superheating of the wall above the saturation temperature is denoted

$$\Delta T_{wSAT} = T_w - T_{SAT}$$

The difference between the wall and fluid temperature is denoted

$$\Delta T_w = T_w - T_f$$

At any axial location Z along the heated channel, the wall temperature is given by the wall heat flux, $q_w(Z)$, the heat transfer coefficient, $h_c(Z)$, and the fluid temperature

$$T_w(Z) = T_f(Z) + \frac{q_w(Z)}{h_c(Z)} \qquad \textbf{Eq. 5-1}$$

The fluid temperature in the discussions herein is the bulk-average fluid temperature. Generally, the fluid temperature adjacent to the wall heating the fluid will be higher than the bulk average temperature. The fluid temperature decreases from the value at the wall to the minimum value in the center of the channel. The effect of unequal liquid and vapor temperatures that may result from certain conservations equations is not considered here.

The fluid and clad-surface temperatures will increase from the channel inlet as the fluid flows along the channel. The wall-to-fluid heat transfer mechanism from the inlet of the channel to the point of onset of nucleation (ONB) will be forced convection between the single-phase liquid and the clad. ONB occurs when the clad surface temperature $T_w(Z)$ is greater than $T_{SAT}(Z)$ by some threshold.

$$T_{wONB}(Z) = T_{SAT}(Z) + (\Delta T_{wSAT})_{ONB} \qquad \textbf{Eq. 5-2}$$

Modeling of the wall superheat threshold required for ONB is discussed later in this section.

Characteristic Macroscopic Length Scale

The rod array geometry has geometric characteristics that lead to ambiguous macroscopic characteristic dimensions at both the array and subchannel levels. A typical array can contain both heated and unheated rods and rods of different diameter. The spaces at the boundaries between arrays introduce subchannels with different dimensions from those within the array. At the grid spacers the flow area and friction properties of the array are also changed from their nominal values and the properties of the bulk motion are affected.

Unlike a simple flow channel such as a round tube, there are several length scales that may be used to characterize the dimension of the fuel rod array in heat transfer and friction factor models and correlations. Todreas and Kazimi [5.1] present detailed discussions of the fuel rod array and it geometric characterization.

The characteristic dimensions typically encountered in models and correlations include the rod diameter, Dr, and the wetted and heated equivalent diameters given by

$$D_{hy} = \frac{4A_f}{P_w} \qquad \textbf{Eq. 5-3}$$

$$D_{he} = \frac{4A_f}{P_h} \qquad \textbf{Eq. 5-4}$$

respectively, where A_f is the flow area, P_w is the wetted perimeter, and P_h is the heated perimeter.

Equations 5-3 and 5-4 can be written in terms of the wetted and heated specific area for the array as follows

$$D_{hy} = \frac{4V_f}{A_w} = \frac{4}{\overline{A}_w} \qquad \textbf{Eq. 5-5}$$

$$D_{he} = \frac{4V_f}{A_h} = \frac{4}{\overline{A}_h} \qquad \textbf{Eq. 5-6}$$

respectively, where V_f is the volume occupied by the fluid and A_w and A_h are the wetted and heated surface area in the array. The specific areas, the wetted and heated surface area per unit fluid volume, $\overline{A}_w$ and $\overline{A}_h$ are used in some mathematical models for descriptions of the rod-array geometry. The specific area is related to the equivalent diameter as shown in Eqs. 5-5 and 5-6.

Modeling of the rod array geometry as porous media has proven to be successful for some correlations for friction factor and heat transfer coefficient. This modeling approach, discussed by Todreas and Kazimi [5.1]will use the specific areas given above.

A third candidate for the characteristic dimension is that given by the equivalent-annulus concept [5.1]. The diameter of the inner rod in the equivalent annulus is taken to be the rod diameter. The inner diameter of the outer tube for the annulus is obtained by letting the flow area for the subchannel be determined by the equation for a flow area bounded by the rod and the fictitious outer tube. The surface of zero shear in the equivalent annulus is determined by the equations for the turbulent velocity distribution in an annulus. The equivalent-annulus concept is presented later in this section.

The uncertainty of the geometric situation is compounded at the subchannel level. The array is composed of central, side, and corner subchannels (the latter two occurring at the boundary between arrays) and subchannels can be bounded by unheated rods and rods of different diameter. Additionally, the flow rate (velocity) and thermodynamic state (pressure and temperature) of the coolant is a function of the radial and axial position within the array. A subchannel model of the thermal-hydraulics in rod arrays is employed to account for variations in the rod-array geometry and distributions of coolant conditions within the array. However, a subchannel model still requires that appropriate characteristic dimensions be determined for use in empirical correlations for friction and heat transfer coefficients. The equivalent diameters and specific areas given above are used for this purpose.

Although there are several candidates for the characteristic dimension in a rod array, whichever is chosen must be used in a consistent manner so that the following relationship applies

$$Nu = St\,Pr\,Re \qquad \textbf{Eq. 5-7}$$

where the Stanton number is

$$St = \frac{h_c}{\rho V Cp} \qquad \textbf{Eq. 5-8}$$

Where ρ is the fluid density, V is the velocity, and Cp the specific heat. Basically, Eq. 5-7 requires that the same characteristic length be used in the Nusselt and Reynolds numbers [5.13].

However, which macroscopic length scale might provide the best characteristic dimension for use in heat transfer coefficient correlations for rod array subchannels is not clear at the present time.

Single-Phase Heat Transfer Coefficient Models and Correlations

Many models and correlations for the single-phase forced-convection heat transfer coefficient for heating a fluid are available and routinely used for engineering analyses of the thermal performance of the PWR core. While a tremendous amount of research has been devoted to develop an understanding of turbulent fluid flow, it is important to note that results from simpler geometries are frequently employed for use in the rod array geometry. There is no theoretical justification for this approach at either the microscopic or macroscopic levels. Almost all these simpler flow channels have convex boundaries relative to the fluid and the boundaries usually form a closed surface, as the inside of a tube. In a fuel-rod array, the heated surface is concave relative to the fluid and there are no closed surfaces bounding the fluid near the heated surface.

The microscopic turbulent velocity and temperature distributions within the fluid in a rod array are not those obtained for round tubes, annuli, or any other simple geometry with closed boundaries. Recent experimental results show that the rod array has its own unique properties relative to turbulence [5.2 - 5.9]. In particular, these recent results have shown that the popular two-parameter models for the turbulence in the flow field are not valid for the rod array geometry. This finding further demonstrates that the usual two-parameter turbulence models applied to many engineering flows are not universal in character. They are engineering models of flow-field properties and not universal models of turbulent fluids. The empirical constants contained in the models are functions of the flow field, not the turbulent fluid.

The unique properties of turbulent flows in rod arrays suggest that application of models and correlations from other geometries cannot be applied to the rod array with any assurance of the accuracy that will result. Application of friction factor and heat transfer coefficient correlations from round tubes and annuli to the rod array cannot be justified on any engineering grounds.

Dittus-Boelter Correlation

The Dittus-Boelter empirical correlation is the most widely used correlation for the single-phase heat transfer coefficient. Being well known, it forms a basis for comparison of predictions with other models and correlations.

The Dittus-Boelter correlation gives the Nusselt number as

$$Nu = 0.023\,Re^{0.80}\,Pr^{0.40} \qquad \textbf{Eq. 5-9}$$

where the exponent on the Prandtl number is for heating of the fluid. In Eq. 5-9 The Nusselt number is

$$Nu = \frac{h_c D_{he}}{k_l} \qquad \textbf{Eq. 5-10}$$

so the heat transfer coefficient is

$$h_c = 0.023\,Re^{0.8}\,Pr^{0.4}\left(\frac{k_l}{D_{he}}\right) \qquad \textbf{Eq. 5-11}$$

where

$$Re = \frac{GD_{he}}{\mu_l} \qquad \textbf{Eq. 5-12}$$

is the Reynolds number, and

$$Pr = \frac{Cp_l \mu_l}{k_l} \qquad \textbf{Eq. 5-13}$$

is the Prandtl number. The heated-equivalent diameter is used as the characteristic dimension. Any of the candidate macroscopic characteristic dimensions given previously could be used.

The Dittus-Boelter correlation was originally developed as an empirical fit to experimental data for flow of water and oils in round tubes under both heating and cooling conditions. For fluid cooling, the exponent on the Prandtl number is 0.30. It is usually stated that the correlation is valid for Reynolds number greater than about 10,000. A summary of the original experimental data on which the Dittus-Boelter correlation is based and other investigations of single-phase heat transfer is given in the RELAP5 [5.10] manual. Most every book or paper that addresses single phase forced convection will provide commentary on their own models along with a comparison to the Dittus-Boelter correlation. Variations in the predicted-experimental wall temperature data may range from 10 to 40%. This illustrates the difficulty in predicting wall temperature even in a simple tube or annulus geometry.

Many variations of the Dittus-Boelter correlation have been developed and used for applications to specific flow-channel geometries and fluid states (various liquids, gases including the vapor phase of liquids, and various flow channel geometries).

Turbulence and the Prandtl Number

In contrast to the empirical fitting of experimental data, analysis of the velocity and temperature fields in a turbulent flow can provide insights into the basic characteristics of momentum and energy exchange between the fluid and a heated solid surface. The momentum exchange is usually expressed in the form of a friction factor and the energy exchange as a heat transfer coefficient.

Analytical studies were started by Prandtl [5.11] for plane shear flows past a horizontal flat plate. In the Prandtl model the flow field adjacent to a solid surface is envisioned to be made up of three regions; (1) a thin laminar sublayer directly adjacent to the stationary surface, (2) a transition region between the laminar sublayer and (3) the fully turbulent region far from the surface. Molecular effects, both viscosity and thermal conductivity, dominate in the laminar sublayer and turbulent effects dominate in the fully turbulent region. Within the transition region both molecular and turbulent effects are important.

Prandtl's original modeling of the turbulent boundary layer was based on a simple linear mixing-length model for the effective turbulent viscosity. In spite of its simplicity, the model has proven to be very effective for analysis of the friction between the fluid and the stationary surface.

Application of the Prandtl mixing-length model to turbulent flows in straight, constant-diameter, round tubes gives the Darcy friction factor for these flows to be

$$\frac{1}{\sqrt{f}} = 2.0\log(Re\sqrt{f}) - 0.8 \qquad \textbf{Eq. 5-14}$$

and this result has proven to provide good predictions of experimental data for flows in smooth channels.

In heated, or cooled flows, the heat transfer coefficient is of interest in addition to the friction factor. The effective turbulent thermal conductivity is usually absorbed into the Prandtl number that arises when the basic Navier-Stokes and energy equations are non-dimensionalized. Models for the variation of the turbulent Prandtl number within the flow field are thus needed to proceed with the prediction of the heat transfer coefficient. Since the time of Prandtl's original model, various extensions and elaborations have been devised attempting to more closely account for the details of the velocity and temperature distributions within the fluid.

If the Prandtl number is large (small molecular thermal conductivity), the main resistance to heat transfer resides in the laminar sublayer. For sufficiently large Prandtl number, the thermal resistance will be completely within the laminar subregion very near the wall of a heated fluid flow and the thermal resistance will be primarily due to conduction. If the Prandtl number is small (large molecular thermal conductivity), the thermal resistance is distributed over the entire

flow cross section. The temperature distribution looks like that obtained in the case of laminar flow. The Prandtl number is important relative to modeling of heat transfer coefficients and analytical solutions of the basic fluid flow equations. The molecular Prandtl number for water varies from less than one at high temperature to about ten at lower temperature.

A brief description of the background for the heat-momentum analogies is given in the following discussion. The discussion given here is based on Kays and Crawford [5.13] and Arpaci [5.20].

Turbulent Transport Coefficients. Recall that the turbulent transport of momentum and heat are usually defined in terms of turbulent transport coefficients analogous to those for molecular fluid properties. The shear stress for a two-dimensional plane shear flow is

$$\tau_{yx} = \rho(\nu + \nu_T)\frac{dU}{dy} \qquad \textbf{Eq. 5-15}$$

and the heat flux is

$$q_y = -\rho C_p(\alpha + \alpha_T)\frac{dT}{dy} \qquad \textbf{Eq. 5-16}$$

In these equations ν is the viscosity, or momentum diffusivity, and α is the thermal diffusivity. The turbulent diffusivities have a subscript, T, and the molecular values do not have a subscript. The turbulent diffusivities are defined by

$$\tau_{yx} = -\rho\overline{u'v'} = \rho\nu_T\frac{dU}{dy} \qquad \textbf{Eq. 5-17}$$

and

$$\frac{q'_y}{\rho C_p} = \overline{v'T'} = -\alpha_T\frac{dT}{dy} \qquad \textbf{Eq. 5-18}$$

Analogous to the molecular properties, a turbulent Prandtl number can be defined

$$Pr_T = \frac{\nu_T}{\alpha_T} \qquad \textbf{Eq. 5-19}$$

Equation 5-15 describes the shear force acting on the fluid parallel to the wall due to velocity gradient normal to the wall and Eq. 5-16 describes the heat flow normal to the wall due to the temperature gradient in that direction. These equations are equally valid for a plane shear boundary layer on a flat plate and for flow inside conduits. Ultimately, the thermal boundary conditions for the surface adjacent to the fluid must also be considered in order to obtain a solution to the complete system of equations that describe the flow. For the present discussion we need only the two equations given above.

Prandtl's mixing length is the usual approach for modeling the momentum, or eddy, diffusivity. Prandtl's mixing-length model for turbulent flows has an analogy with the kinetic theory of gases. In the kinetic theory the molecular diffusivity of momentum is proportional to the mean-free-path and the root-mean-square velocity of the molecules. For turbulent flows, Prandtl assumed the turbulent diffusivity to be proportional to the product of a mixing length and a characteristic velocity of the turbulent fluctuations. The physical processes and their scales are basically different. Molecular momentum transfer in a gas is characterized by a large number of small identifiable particles, the molecules, exchanging momentum through discrete interactions by collisions. Turbulent momentum transfer is characterized by a much smaller number of large and poorly defined fluid eddies exchanging momentum through continuous interactions. The fluid eddy interaction includes the effects of pressure fluctuations on the momentum transfer. A process that does not have a counterpart in the kinetic theory of gases.

The continuous interactions between the fluid eddies, or chunks of material, exchange momentum and energy completely independent of that transferred by molecular processes. The momentum exchange is due to pressure forces acting on the fluid eddy as a result of contact with the surrounding fluid. Viscous stresses are present, but they must be small. Recall that the turbulent Reynolds stresses arise from the basic Navier-Stokes equations from the momentum flux terms on the left-hand side of the local-instantaneous equations. The molecular viscous stresses are on the right-hand-side of the equations and do not enter the development of the turbulent Reynolds stresses. The corresponding energy exchange between the eddies and surrounding material is by heat conduction, because there are mechanisms for heat transfer analogous to the pressure forces in momentum exchange.

The Reynolds Analogy. The Reynolds analogy between heat and momentum exchange is obtained as follows. Assume that a steady fully-developed turbulent flow exists in a straight simple flow channel. The flow field is made up of two parts; a wall layer of thickness δ and a turbulent core extending from δ to the center of the channel. The velocity varies from zero at the wall to the bulk-mean value U_m at δ and is uniform δ to the center line. The fluid temperature varies from T_w at the wall to the bulk-mean value T_m at δ and is uniform from δ to the center line. The ratio of Eqs. 5-15 and 5-16 integrated over the wall layer is

$$\frac{\tau_w / \rho}{q_w / \rho C_p} = \left[\frac{\nu + \nu_T}{\alpha + \alpha_T}\right]\left[\frac{U_m}{T_w - T_m}\right] \qquad \textbf{Eq. 5-20}$$

based on the assumption that the ratios of both fluxes and diffusivities are constant.

Using the heat transfer coefficient defined by

$$q_w = h_c(T_w - T_m) \qquad \textbf{Eq. 5-21}$$

and the Stanton number defined by

$$St = \frac{h_c}{\rho C_p U_m} \qquad \textbf{Eq. 5-22}$$

and the friction factor

$$f_w = \frac{\tau_w}{\frac{1}{2}\rho U_m^2} \qquad \textbf{Eq. 5-23}$$

Eq. 5-20 can be written

$$St = \frac{1}{2} f_w \frac{\alpha + \alpha_T}{\nu + \nu_T} \qquad \textbf{Eq. 5-24}$$

or,

$$St = \frac{1}{2} f_w \frac{\alpha / \alpha_T + 1}{\nu / \alpha_T + \nu_T / \alpha_T} \qquad \textbf{Eq. 5-25}$$

Equation 5-25 shows that if (1) the turbulent diffusivities are very much bigger than the molecular diffusivities and (2) the turbulent Prandtl number, $\nu_T/\alpha_T = 1.0$ then

$$St = \frac{1}{2} f_w \qquad \textbf{Eq. 5-26}$$

Equation 5-26 is the Reynolds analogy between heat and momentum exchange.

The first assumption means that the effects of the wall layer have been neglected and the second assumption means that the difference between the physical processes of momentum and energy exchange have been neglected.

The Prandtl Analogy. The Prandtl analogy improves on the Reynolds analogy by incorporating direct accounting for the viscous wall layer. In the wall layer the molecular diffusivities dominate the physical processes and the turbulent effects can be neglected. In the turbulent core the turbulent processes dominate and the molecular effects can be neglected. The ratio of Eqs. 5-15 and 5-16 is integrated across each region separately, applying the assumptions just listed and the solutions coupled at the interface located at d. Arpcai [5.20] gives the Prandtl analogy results

$$St = \frac{1}{2} f_w \left[\frac{1/Pr_T}{1 + \frac{U_\delta}{U_m}\left(\frac{Pr}{Pr_T} - 1 \right)} \right] \qquad \textbf{Eq. 5-27}$$

where U_δ is the fluid velocity at the edge of the viscous layer. Arpaci notes that generally Pr_T is taken to be 0.90 and that the velocity ratio in the denominator can be written in terms of wall-coordinate variables. Using that information, Eq. 5-27 can be written

$$Nu = \frac{1.11\frac{f_w}{2} Re\, Pr}{1+11.6\left(\frac{f_w}{2}\right)^{1/2}(1.11Pr-1)}$$ **Eq. 5-28**

Prandtl and Colburn Analogy

Because the Prandtl number enters analytical solutions for the heat transfer coefficient, special cases can be determined by setting the Prandtl number to large or small values. A Prandtl number of one corresponds to the Reynolds analogy between momentum and heat transfer [5.12, 5.13]. The Reynolds analogy thus neglects the effects of the differences between momentum and heat transport within the fluid. Momentum transport due to a pressure-difference potential is assumed to be analogous to heat transport and its associated temperature-difference potential. Kays [5.12] and Kays and Crawford [5.13] give details of the Reynolds analogy and its shortcomings in this respect.

The Reynolds analogy gives the relationship between the friction factor and the heat transfer coefficient to be

$$\frac{h_c}{\rho C_p V} = \frac{f_w}{2}$$ **Eq. 5-29**

where h_c is the convective heat transfer coefficient, V is the average flow speed, and f_w is the Fanning wall friction factor. Note that because of the basis for the analogy the Prandtl number doesn't enter Eq. 5-29.

The quantity on the left-hand side of Eq. 5-29 is the Stanton number

$$St = \frac{Nu}{Re\, Pr}$$ **Eq. 5-30**

so Eq. (5-29) is

$$Nu = \left(\frac{f_w}{2}\right) Re\, Pr$$ **Eq. 5-31**

Any appropriate correlation for the wall friction factor can be used in these equations and those given below. Generally, textbooks and papers use the McAdam form for flows in round tubes

$$f_w = 0.046\, Re^{-0.20}$$ **Eq. 5-32**

for higher ranges of the Reynolds number, 30,000 < Re < 1.0 x 10^6, and the Blasius empirical equation

$$f_w = 0.079\,Re^{-0.25} \qquad \textbf{Eq. 5-33}$$

for lower ranges of the Reynolds number, 5000 < Re < 30,000. Prandtl's results of Eq. 5-14 could just as well be used in place of either of these.

Note that putting Eq. 5-32 or Eq. 5-33 into Eq. 5-31 will give different dependencies of the Nusselt number on the Reynolds number. The Reynolds analogy gives the Nusselt number to be a function of the Prandtl number to the 1.0 power. Also note that these friction factor and heat transfer coefficient correlations are usually generalized to non-circular geometries in the engineering literature by use of the heated and wetted equivalent diameters; Eq. 5-3 for the wetted equivalent diameter, and Eq. 5-4 for the heated equivalent diameter. There is no theoretical basis for the use of either of these.

Kays and Crawford [5.13] and Arpaci [5.20] credit Colburn with removing some of the limitations associated with the Reynolds analogy. The Colburn analogy is empirical, but Arpaci [5.20] has derived the analogy based on the microscales of turbulence. The Colburn analogy is

$$St = \left(\frac{f_w}{2}\right)\frac{1}{Pr^{2/3}} \qquad \textbf{Eq. 5-34}$$

for the Stanton number which gives the Nusselt number to be

$$Nu = \left(\frac{f_w}{2}\right) Re\, Pr^{1/3} \qquad \textbf{Eq. 5-35}$$

Putting an equation for the wall friction factor into Eq. 5-35 will give the basic form of the Dittus-Boelter correlation for cooling a liquid. Equation 5-32 gives

$$Nu = 0.023 Re^{0.8}\, Pr^{1/3} \qquad \textbf{Eq. 5-36}$$

Note that the momentum-energy analogies do not differentiate between heating and cooling a single-phase liquid.

Kays and Co-workers

Kays [5.12], was among the first to systematically investigate analytically the effects of the Prandtl number on heat transfer coefficients. The most recent edition of Kays' book is [5.13]. His heat transfer textbook contains a complete discussion of how the momentum and thermal boundary layers interact and how the Prandtl number enters analytical solutions for the heat transfer coefficient. Kays and Leung [5.14] have given the standard model for heated flows in annuli.

Kays' [5.12] result based on the standard three-region velocity distribution without any smoothing factors is

$$Nu = \frac{\left(\frac{f_w}{2}\right)^{1/2} Re\,Pr}{0.833\left[5\,Pr + 5\ln(5\,Pr+1) + 2.5\ln\left(\frac{\left(\frac{f_w}{2}\right)^{1/2} Re}{60}\right)\right]} \qquad \text{Eq. 5-37}$$

Note that Eq. 5-37, gives a dependency on the Reynolds number in the numerator that is different from the usual dependency. Putting Eq. 5-32 into the numerator of Eq. 5-37 will give an exponent of 0.90 for the Reynolds number. Kays says Eq. 5-37 is in good agreement with experimental data for Prandtl number range of 0.50 to 30.0, which includes the liquid phase of water.

The most recent edition of the Kays book [5.13] gives

$$Nu = \frac{\left(\frac{f_w}{2}\right) Re\,Pr}{0.88 + 13.39\left(\frac{f_w}{2}\right)^{1/2}(Pr^{2/3} - 0.78)} \qquad \text{Eq. 5-38}$$

based on an empirical fit for the temperature distribution in turbulent flow at Prandtl numbers of Pr = 0.70 and Pr = 5.9. This range of Prandtl number is close to the values for subcooled water.

Petukhov and Co-workers

Petukhov and his co-workers [5.15 - 5.18] have given a generalized result, based on numerical calculations and experimental data, for the heat transfer coefficient for flows in round tubes for wide ranges of Prandtl Number. Petukhov and his co-workers, among others, have extended the work done by Kays to wider ranges of operating conditions and fluid states and improved the accuracy of heat transfer coefficient correlations. The Nusselt number is

$$Nu = \frac{\left(\frac{f_w}{2}\right) Re\,Pr}{K_1(f_w) + K_2(Pr)\left(\frac{f_w}{2}\right)^{1/2}(Pr^{2/3} - 1)} \qquad \text{Eq. 5-39}$$

where

$$K_1(f_w) = 1.0 + 3.4 f_w \qquad \textbf{Eq. 5-40}$$

$$K_2(Pr) = 11.7 + 1.8 / Pr^{1/3} \qquad \textbf{Eq. 5-41}$$

The ranges covered by Eq. 5-39 are $10^4 < Re < 5.0 \times 10^6$ and $0.5 < Pr < 2000.0$ with 1 - 2% accuracy for heat transfer in round tubes [5.16]. The model is based on very detailed accounting for turbulence effects on the velocity and temperature distributions within the fluid by using the Reichardt and Deissler models [Petukov, 5.16] for distribution of the momentum and heat eddy diffusivity. By assuming a plane shear flow, a system of ordinary differential equations requiring numerical methods for solution is obtained. The modeling does not account for induced secondary flows and bulk motion transverse to the primary flow direction such as may be present in a rod array. It is doubtful that a two-dimensional, plane, shear-flow description of the three-dimensional flow in a rod array is correct; turbulence is in general always three-dimensional having random motions in all three coordinate directions.

A form of Eqs. 5-39 through 5-41 said to be accurate within 5-6% that can be used for engineering calculations is

$$Nu = \frac{\left(\frac{f_w}{2}\right) Re\, Pr}{1.07 + 12.7\left(\frac{f_w}{2}\right)^{1/2} (Pr^{2/3} - 1)} \qquad \textbf{Eq. 5-42}$$

Gnielinski [5.19] has specialized Eq. 5-42 to better handle the lower range of the Reynolds number to the form

$$Nu = \frac{\left(\frac{f_w}{2}\right) (Re - 1000.0)\, Pr}{1.07 + 12.7\left(\frac{f_w}{2}\right)^{1/2} (Pr^{2/3} - 1)} \qquad \textbf{Eq. 5-43}$$

These results from the momentum-heat analogy and approximate analytical models are important because more is generally known about the wall friction factor than about the heat transfer coefficient. Experimental data for the friction factor can be used to estimate the heat transfer coefficient. Given the still approximate basis for the analytical models, however, rather than eliminating experimental heat transfer data completely, the results can be used to both guide heat transfer testing and check the experimental data with the analytical results.

Microscales of Turbulence

Arpaci [5.20], has presented a method of modeling friction and heat transfer by considering the microscales in turbulent flows. There may be some hope that the small-scale motions in turbulent flows are somewhat universal in nature and thus results based on these may have wide applicability. For the heat transfer coefficient in turbulent flows Arpaci gets

$$Nu = \left(\frac{f_w}{2} \right) Re\, Pr^{1/3}\, \Phi(Re,Pr) \qquad \textbf{Eq. 5-44}$$

where

$$\Phi = \frac{1 + \dfrac{C}{Re^{1/4}}}{1 + \dfrac{C}{Re^{1/4}\, Pr^{1/3}}} \qquad \textbf{Eq. 5-45}$$

The numerical value for C is obtained from experimental data. Arpaci shows that Eq. 5-44 gives Nusselt numbers between those from the Reynolds and Colburn analogy.

Equivalent Annulus

Todreas and Kazimi [5.1] recommend that an equivalent-annulus model for the rod array subchannel provides a good characteristic dimension for use in friction and heat transfer correlations valid for turbulent flow but developed from experimental data other than from rod arrays. In the equivalent-annulus model the rod array subchannel is mapped to an annulus in which the flow area of the subchannel is equated to that of an annulus. The rod diameter is taken to be the diameter of the inner rod in the annulus. The inner diameter of the outer rod of the annulus is given by the usual equation for the flow area in an annular channel. The surface of zero shear is also determined by the flow rate in the subchannel. The details of the modeling approach are given in [5.1], and are not repeated here. There is no evidence to show that this approach improves the accuracy of the closed channel models when applied to rod array subchannels.

An interesting result is obtained from the equivalent-annulus model as shown in the following example.

Donne and Meerwald [5.21] have given a version of the Petukhov and Roizen correlation [5.17] for flow in a heated annulus as

$$Nu = 0.018 \left(\frac{D_o}{D_i} \right)^{0.16} Re^{0.80}\, Pr^{0.40} \qquad \textbf{Eq. 5-46}$$

Equation 5-46 can be used with the equivalent-annulus concept to get a handle on how the rod bundle geometry may impact the heat transfer coefficient correlation. The rod diameter is used for D_i. The equivalent annulus model determines the D_o to be used as follows. The flow area associated with a central subchannel in a rod array with square pitch is

$$A_f = D_i^2\left[\left(\frac{P}{D_i}\right)^2 - \frac{\pi}{4}\right] \qquad \textbf{Eq. 5-47}$$

where P is the rod-to-rod pitch. The outer diameter of the equivalent annulus is given by this flow area as follows

$$D_o = D_i\left(\frac{4}{\pi}\right)^{1/2}\left(\frac{P}{D_i}\right) \qquad \textbf{Eq. 5-48}$$

For typical values of rod diameter, 10.0 mm (0.394 in), and pitch-to-diameter ratio of 1.3, the outer diameter of the equivalent annulus from Eq. 5-48 is about, D_o = 14.67 mm (0.58 in). Putting these values into Eq. 5-46 gives

$$Nu = 0.0191\,Re^{0.80}\,Pr^{0.40} \qquad \textbf{Eq. 5-49}$$

a value that is approximately 20% less than the standard Dittus-Boelter correlation. The equivalent-annulus approach indicates that the heat transfer coefficient for a subchannel will be less than that from a round tube.

Empirical Correlations and the Prandtl Number

Kays in the first edition of his book [5.12] provides a collection of heat transfer coefficient correlations that is a function of the range on the Prandtl number. The correlations he gives for 1.0 < Pr < 20.0 (water and light liquids) is

$$Nu = 0.0155\,Re^{0.83}\,Pr^{0.50} \qquad \textbf{Eq. 5-50}$$

Note that Eq. 5-50 is not the usual Dittus-Boelter correlation. The dependency of the Nusselt number on the Prandtl number corresponds to a surface-renewal model of the heat transfer process. The basis of the surface-renewal model is that the energy exchange is dominated by conduction into a liquid suddenly exposed to the clad surface temperature.

The latest edition of Kays [5.13] no longer includes the compilation of correlations, but the authors conclude that the Dittus-Boelter correlation tends to overpredict the Nusselt number for gases by at least 20%, and to underpredict the Nusselt number for higher-Prandtl-number fluids by 7 to 10%. The correlation is not recommended for use.

Comparison Charts

Figures 5-1and 5-2 present a comparison of the Kays Eq. 5-38 , Petukov Eq. 5-39, and Gnielinski Eq. 5-43, models used with the Dittus-Boelter correlation used as the base. Figure 5-1 is based on a Prandtl number of 1.0 which is typical of high temperature water where Figure 5-2 is based on a Prandtl number of 10 which is typical of cooler water. The comparison in both of the figures shows all of the models are similar in their difference with Dittus-Boelter. The Gnielinski model exhibits odd characteristics at lower Reynolds numbers because of the use of 1000 as a reference value within the model. For the Prandtl number of 1.0, the magnitude of the deviation (~5%) is not that remarkable. The difference at the large Prandtl number becomes quite significant at higher Reynolds numbers.

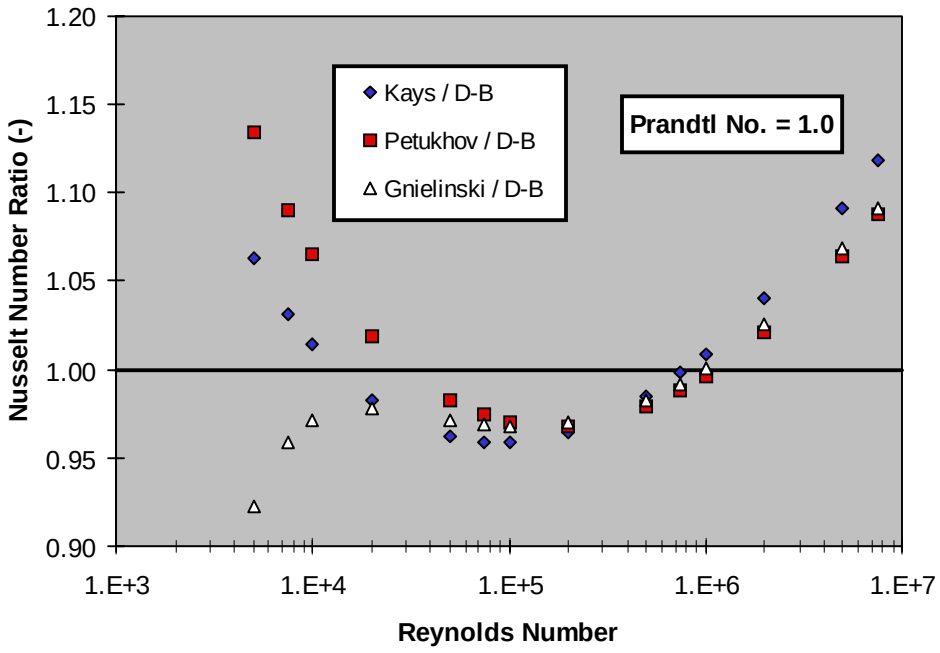

Figure 5-1
Nusselt Number Ratio for Prandtl Number = 1

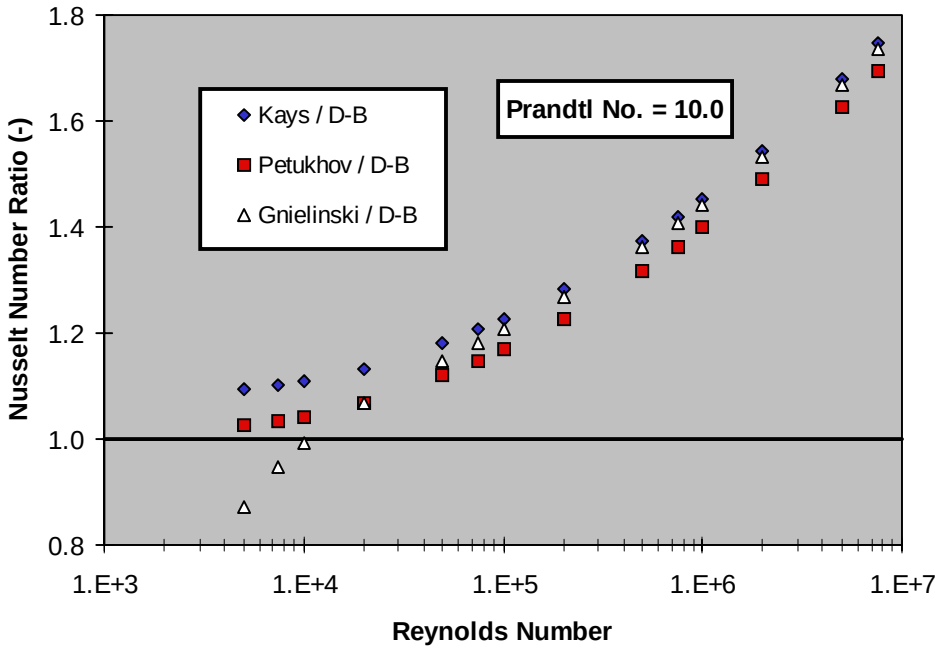

Figure 5-2
Nusselt Number Ratio for Prandtl Number = 10

Boiling Heat Transfer Correlations and Models

Boiling Heat Transfer Regimes

The heat transfer regimes of interest are shown in Figure 5-3, which is based on Figure 5.1 of Collier and Thome [5.22]. The figure shows a boiling flow in a straight heated channel with subcooled liquid fed to the inlet. The top part of the figure shows representations of the distribution of the vapor within the flow channel from the point of ONB to fully developed saturated boiling. The bottom part of the figure shows representative fluid and wall temperature distributions. These are given for the case of uniform heat addition to the fluid as a function of distance from the channel inlet. For this case, the fluid and surface temperature increase linearly along the channel.

The exact distributions for the case of non-uniform heating will be different, but that has no effect on the following discussion. The ONB and FDB locations are of interest to in the following discussions. Partial subcooled boiling (PSB) occurs between these locations.

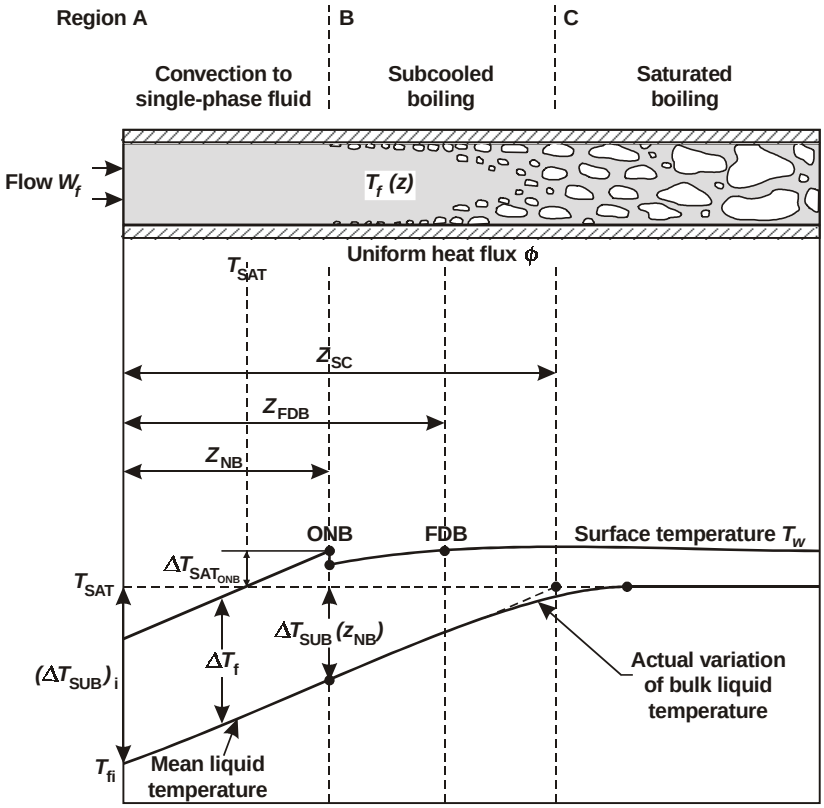

Figure 5-3
Subcooled Boiling Heat Transfer Regimes

Onset of Nucleate Boiling and Partial Subcooled Boiling. The fluid temperature increases from its value at the channel inlet as the fluid flows past the heated surface. When the clad surface is sufficiently superheated, then nucleation begins and the very large heat transfer coefficient may cause the clad surface temperature to decrease. ONB occurs where the clad surface temperature equals $T_{wONB} = T_{SAT}(P) + (\Delta T_{wSAT})_{ONB}$. At ONB, vapor bubbles are generated in the microscopic cracks and crevices in the clad surface. The bubbles will grow and collapse at the active nucleation sites although some may slide along the surface pulled along by the drag between the liquid and vapor. At the very small distances from the surface in which the bubbles are present, possibly in the laminar sublayer, the fluid velocity is small and thus the drag force will be small.

At the ONB location only a few isolated nucleation sites will be active and the bubbles will grow and collapse with little interference from other bubbles. Downstream from ONB, as the superheat of the fluid adjacent to the clad and the clad surface increases, more nucleation sites will become active and more of the surface will be covered with vapor. The heat transfer mechanisms thought to be important in the PSB regime are evaporation of a very thin micro-layer of liquid between the clad surface and the bubble and convection and conduction between the vapor and liquid along the surface of the bubble. Recondensation of the vapor back into the liquid occurs when the bubble grows into the subcooled liquid away from the wall. Additionally, the action of vapor generation and collapse on the clad surface are thought to increase the convective component of heat transfer. Within the PSB regime, many models of the heat transfer

are based on superposition of convective and boiling contributions. These correlations will be discussed later in this section. Some of the clad-to-fluid heat transfer occurs as convective heat transfer between the patches of bubbles on the clad surface.

Fully Developed Subcooled Boiling. Fully developed subcooled boiling (FDSB) occurs somewhere between ONB and bulk saturated nucleate boiling (SNB). The definition of FDSB is somewhat subjective. As shown in Figure 5-3, FDB is close to where a significant number of bubbles begin to depart from the wall and migrate into the bulk liquid. FDSB may correspond to the onset of significant void (OSV). The OSV has been of recent interest because of its role in the stability of two-phase flows in heated channels at lower flow rates. A review has been given by Lee and Bankoff [5.23].

At FDB (Figure 5-3), almost all the heat transfer between the clad surface and the fluid is due to the boiling process. Many nucleation sites are active and the clad surface is more or less covered by vigorously boiling vapor and liquid microlayers under the bubbles. The heat transfer coefficient is large and is more or less independent of the flow rate of the fluid. Also, as shown in Figure 5-3 the wall superheat reaches an almost constant value at the location of FDSB.

There are several ways that the heat transfer coefficient is modeled and correlated in the PSB and FDSB regimes. In one approach, no distinction is made between these regimes. The model and correlation is applicable to both regimes. Additionally, some of these correlations will be applicable to the bulk saturated nucleate boiling (SNB) regime. In the second approach, the existence of the PSB regime as a distinct heat transfer regime is explicitly modeled. The resulting correlations, however, are heuristic and rely on correlations for the heat transfer coefficient in subcooled forced convection and in the FDSB regime.

Bulk Saturated Nucleate Boiling. Saturated bulk boiling starts when the channel-average fluid temperature reaches the saturation temperature corresponding to the local pressure. As shown in Figure 5-3, the bulk liquid temperature reaches the saturation temperature a little downstream of where the energy equation would predict. The difference is the part of the wall heat flux that has gone into production of vapor.

Modeling and correlations for ONB, PSB, and FDSB are discussed in the following paragraphs.

ONB Models and Correlations

The criterion for ONB determines the location along the heated wall where vapor nucleation begins to occur in microscopic crevices on the wall surface. Generally the wall temperature will be greater than the saturation temperature of the fluid and thus there is a region in the fluid just adjacent to the wall in which the liquid is superheated. Detailed discussion of the models and correlations for ONB have been given by Collier and Thome [5.22], Carey [5.24] and Whalley [5.25].

Only a few of the available models will be discussed here. The wall superheat required to initiate nucleation at high pressure decreases and may be only 1°C (2°F) at PWR operating conditions. Given that the forced convection temperature difference will be on the order of 25°C (40°F), it makes little sense to spend a great deal of effort on the wall superheat threshold.

None of the models and correlations have been based on, or validated with, experimental data from rod arrays. While the ONB process is primarily a local process, occurring at the level of the microscopic nucleation sites on the clad surface, the geometry of the heated surface enters indirectly through the velocity and temperature distribution within the fluid adjacent to the clad. The status of turbulent flows in rod arrays was discussed in Section 4, Review of Rod Bundle Hydrodynamics and Heat Transfer References. As shown there, it is not clear that the standard universal velocity distribution that is valid for simple closed channels is appropriate for the rod array.

Simplest Model. The most simple and straightforward model is to assume that ONB corresponds to $T_w = T_{SAT}$. As mentioned above, at high pressure the wall superheat needed for ONB is reduced so that making this assumption is somewhat justified. Additionally, given the uncertainty in the accuracy of models and correlations for ONB, and subsequent boiling heat transfer coefficients, taking this assumption makes some sense.

The Standard Model. The model that is almost universally used for prediction of ONB is based on the work of Hsu [5.26]. Hsu's original investigations were for the initiation of boiling on small surfaces in stagnant pools in which conduction and natural convection dominate in the liquid prior to ONB. The modeling approach has been taken to the forced-convection case by Bergles and Rohsenow [5.27] and subsequently extended by Davis and Anderson [5.28]. Collier and Thom [5.22] and Carey [5.24] indicate that Frost and Dzakowic further included accounting for Prandtl number effects. Lee, et al developed an extension of the Hsu model and demonstrated good agreement with their own high pressure data in 1988 [5.46].

The bases for the ONB model is that under some conditions the liquid adjacent to the clad will be sufficiently superheated that a bubble which is growing out of a crevice will not completely recondense. Thus, the surface under consideration must have nucleation sites that are active and out of which vapor bubbles grow into the liquid. Hsu, Bergles and Rohsenow, and Davis and Anderson argue that commercial surfaces almost always meet this requirement because of the wide range of sizes of potential nucleation sites present on these surfaces. A highly-polished surface, on the other hand, may not meet this requirement.

There are two modeling aspects associated with the temperature distribution in the liquid adjacent to the clad. The first is the actual shape of the distribution and the second is at what distance from the clad surface does the liquid need to be superheated. As for the temperature distribution, it must be assumed that at the ONB location the nucleation site density is sufficiently small that bubbles do not affect the temperature, and velocity, distribution. Additionally, it must be assumed that the process which dominates vapor growth at ONB are thermal processes in the fluid. The hydrodynamics forces acting on the vapor bubbles must be sufficiently small to prevent detachment of the bubbles from the cavity. There is significant uncertainty associated with modeling the forces acting on bubbles, therefore trying to introduce this refinement is not justified.

The actual shape of the bubbles growing out of the cavity and the mechanisms responsible for keeping them attached to the clad surface are not known. It is usually assumed that vapor production occurs at the bottom of the bubble through the microscopic liquid layer between the bubble and the clad surface. The actual shape of the bubble, however, may be such that the micro-layer doesn't exist. Vapor production can also occur around the part of the bubble that is

within the superheated liquid layer. Recondensation of the vapor back into the subcooled liquid is usually assumed to occur at the top of the bubble as it grows and moves into the subcooled liquid outside the superheat layer. Whatever the shape of the bubble as it grows and the forces acting on it, these are neglected in the standard analysis.

At the present time, the potential effects of deposits on the clad surface are neglected. This, most likely, is not a good assumption. The potential for significant effects of the deposits on the ONB process is large. The deposits may both increase and enhanced the available nucleation sites enabling greater vapor generation at the same location and wall temperature.

Many of the assumptions listed above could be relaxed and a more nearly complete model developed. Since the time the modeling approach was first devised by Hsu, studies into the many various individual aspects of the model have been conducted. The results of these could be factored into a newer updated model. The resulting model would more likely than not require numerical solution and would thus be somewhat limited in its usefulness compared to the closed solutions available for the more standard models.

Hsu's modeling is based on the conditions required for a bubble to grow in a superheated liquid. The basic assumption is that the bubble will grow if the lowest temperature on the surface of the bubble is greater than that required for nucleation in the cavity. The temperature gradient in the liquid is taken to be linear.

$$T_l(y) = T_w - \left(\frac{q_w y}{k_l} \right) \qquad \textbf{Eq. 5-51}$$

where *y* measures the distance from the clad surface. Equation 5-51 represents the assumption that the heat transfer in the liquid is governed by conduction; i.e.

$$q_w = -k_l \frac{dT_l}{dy} \qquad \textbf{Eq. 5-52}$$

The liquid temperature on the left-hand side of Eq. 5-51 must be greater than saturation temperature at the top of the bubble.

Using the assumptions and approximations listed above, Bergles and Rohsenow obtained the relationship between the wall heat flux and the wall superheat needed for the onset of nucleation to be

$$(\Delta T_{wSAT})_{ONB} = 0.556 \left[\frac{q_{wONB}}{1082 P^{1.156}} \right]^{0.463 P^{0.0234}} \qquad \textbf{Eq. 5-53}$$

where the units are °C for $(\Delta T_{wSAT})_{ONB}$, W/m^2 for q_{wONB} and bar for the pressure, *P*. In engineering units the equation is

$$q_{wONB} = 15.60(\Delta T_{wSAT})_{ONB}^{(2.30/P^{0.0234})} \qquad \textbf{Eq. 5-54}$$

where the units are °F for $(\Delta T_{wSAT})_{ONB}$, Btu/hr ft^2 for q_{wONB}, and psia for the pressure, P.

The Bergles and Rohsenow equation is valid only for water in the pressure range 15 to 2000 psia (0.1 to 13.8 MPa).

Davis and Anderson obtained an analytical solution for the relationship in the form

$$(\Delta T_{wSAT})_{ONB} = \left[\frac{8\sigma q_{wONB} T_{SAT}}{h_{fg} k_l \rho_v}\right]^{0.5} \qquad \textbf{Eq. 5-55}$$

where σ is the surface tension, h_{fg} is the heat of evaporation, k_l is the thermal conductivity of the liquid, and ρ_v is the density of the vapor phase. Equation 5-55 is an approximate solution which is valid for high pressure such as occurs in PWRs at steady-state operating conditions.

The Bergles and Rohsenow and Davis and Anderson equations are shown in Figure 5-4 for two values of the pressure. The results in the figure show the small values of wall superheat needed for nucleation at the high operating pressure for PWRs.

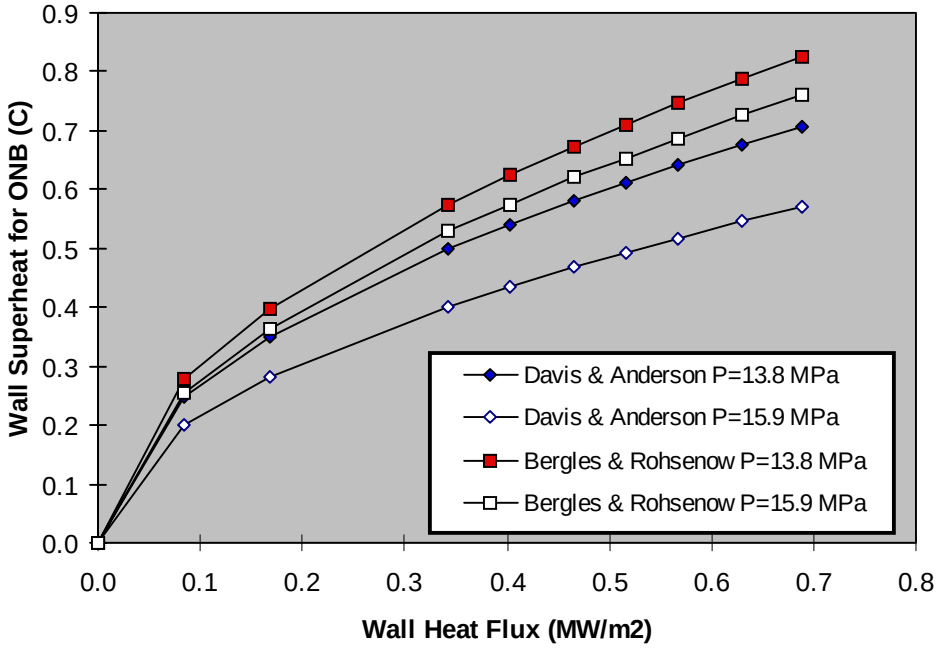

Figure 5-4
Comparison of Bergles & Rohsenow With Davis & Anderson

Partial Subcooled Boiling Models and Correlations

Downstream from the ONB location, superheating of the liquid adjacent to the clad and the clad surface, and the vapor generation rate continue to increase. These conditions result in more nucleation sites becoming active and recondensation of the generated vapor decreasing. The generated vapor is confined to a very thin region near the clad until departure starts near the FDSB location. At the high operating pressure of PWRs, the vapor density is quite large and thus the volume occupied by the vapor is expected to be very small.

Single-phase convective heat transfer occurs up to the ONB location. The heat transfer coefficient between the fluid and clad surface will increase downstream from the ONB location. The dominant mode of heat transfer will vary from single-phase convection near ONB to nucleate boiling as FDSB is approached. The boiling process is very efficient for removing heat from the fuel rods and the clad surface temperature will be very near the saturation temperature for the water at the local pressure. As the clad surface and the fluid superheat increase, the active nucleation site density increases and the nucleate boiling contribution to the heat transfer increases. As will be shown below, several models and correlations for the heat transfer

coefficient in the PSB regime are based on the superposition of forced convection and pool nucleate boiling models and correlations.

The region between the ONB location and the location at which fully developed subcooled boiling (FDSB) starts is denoted the partial subcooled boiling (PSB) regime. Fully developed subcooled boiling is somewhat subjectively set as the location at which there is a significant increase in the nucleate boiling component and vapor bubbles begin to depart from the clad surface. Various modeling approaches have been used to get the heat transfer coefficient in the PSB regime; some quite elaborate.

Some of the PSB models need the heat transfer coefficient for the FDSB regime. The Jens-Lottes [5.29] and Thom [5.30] correlations for FDSB give the wall superheat as a function of the heat flux and pressure. These correlations can be written in the general form

$$(\Delta T)_{wSAT} = (T_w - T_{SAT}) = \Psi q_w^n \qquad \textbf{Eq. 5-56}$$

Another correlating form used in the PSB regime, and the FDSB and bulk saturated boiling regimes, sums the contributions due to forced convection and nucleate boiling in the form

$$q_w = q_{FC} + q_{NB} \qquad \textbf{Eq. 5-57}$$

The driving potential for the two different heat transfer modes is different. The forced-convection contribution is generally assigned the wall-to-bulk fluid temperature potential and the nucleate boiling component is assigned the wall-to-saturation superheat. With these temperature potentials and the heat transfer coefficients, Eq. 5-57 is written

$$q_w = h_c(T_w - T_f) + h_{NB}(T_w - T_{SAT}) \qquad \textbf{Eq. 5-58}$$

The forced convection heat transfer coefficient is usually determined with a modification to the Dittus-Boelter correlation. The nucleate boiling component is usually based on a pool nucleate boiling correlation. The nucleate boiling correlation may be in the form of Eq. 5-56.

Simple Models. The simplest modeling approach is to ignore the partial subcooled boiling regime and assume the single-phase liquid regime exists up to the fully developed subcooled boiling regime. With this assumption, the location of the onset of nucleate boiling is given by the condition

$$(T_w)_{SPL} = (T_w)_{FDSB} \qquad \textbf{Eq. 5-59}$$

If the FDSB correlation is in the form of Eq. 5-56, Eq. 5-59 gives

$$T_f(Z) + \frac{q_w}{h_{cSPL}} = T_{SAT} + \Psi q_w^n \qquad \textbf{Eq. 5-60}$$

Equation 5-60 can be written in the form of a fluid subcooling condition as

$$(\Delta T)_{fSUB} = \left[\frac{q_w}{h_{cSPL}} - \Psi q_w^n \right] \qquad \textbf{Eq. 5-61}$$

A second simple modeling is to assign a fraction of the total heat flux to be the forced convection contribution. This fraction then goes to zero as the FDSB regime is reached. The Bowring [5.31] model is based on this approach.

Correlated Models. As mention above, there are several correlations in the form of Eq. 5-58 that have been developed for both subcooled and saturated boiling. Generally, these full-range correlations do not differentiate between PSB and FDSB, and some do not differentiate between subcooled and saturated boiling. Additionally, some do not differentiate between fully developed nucleate boiling and the forced-convection vaporization regime in which nucleation within the liquid film adjacent to the clad surface is suppressed. The heat transfer regimes for which the correlations are valid are implicitly set by the experimental data on which they are based.

The well-known Jens-Lottes [5.29] and Thom [5.30] correlations are examples of correlations that are valid for only the FDSB heat transfer regime. The Chen correlation [5.32, 5.33], originally developed for saturated boiling is an example of those that are applied for both nucleate boiling and forced-convection vaporization. These and other correlations based of Eq. 5-58 are reviewed in the following discussion.

Fully Developed Subcooled Boiling Correlations

Several correlations of experimental data for the heat transfer coefficient for the fully developed subcooled boiling regime are given in the following discussion. Detailed discussion of many of the models and correlations for fully developed subcooled boiling have been given by Collier and Thome [5.22], Carey [5.24] and Whalley [5.25]. Only a few of these will be discussed here.

Generally, the heat transfer coefficient for fully developed subcooled boiling is at best a weak function of the flow rate of the fluid. Experimental data show that the pressure and wall-superheat level are the primary variables in this heat transfer regime. Both the Jens-Lottes [5.29] and Thom [5.30] correlations reflect this dependency.

Jens-Lottes Correlation. The Jens-Lottes correlation is a dimensional correlation valid only for water. The correlation is based on experimental data for boiling water flowing vertically upward in round tubes. The correlation is

$$(\Delta T)_{wSAT} = 25 q_w^{0.25} e^{-P/62} \qquad \textbf{Eq. 5-62}$$

where the unit for pressure, P, is bar, for $(\Delta T)_{wSAT}$ is C, and MW/m^2 for q_w. In Engineering units the correlation is

$$(\Delta T)_{wSAT} = 1.9 q_w^{0.25} e^{-P/900} \qquad \textbf{Eq. 5-63}$$

where the pressure, P is in psia, q_w is in Btu/hr ft^2, and $(\Delta T)_{wSAT}$ is in F.

Thom Correlation. The Thom correlation is a dimensional correlation valid only for water. The correlation is based on experimental data for boiling water flowing vertically upward in round tubes and annuli. The correlation is

$$(\Delta T)_{wSAT} = 22.65 q_w^{0.5} e^{-P/87} \qquad \textbf{Eq. 5-64}$$

where the unit for pressure, P, is bar, for $(\Delta T)_{wSAT}$ is °C, and MW/m^2 for q_w. In Engineering units the correlation is

$$(\Delta T)_{wSAT} = 0.072 q_w^{0.5} e^{-P/1260} \qquad \textbf{Eq. 5-65}$$

where the pressure, P is in psia, q_w is in Btu/hr ft^2, and $(\Delta T)_{wSAT}$ is in °F.

Note that the Thom and Jens-Lottes correlations have completely different powers on the wall heat flux, and equivalently, the wall superheat.

Chen Correlation. The Chen correlation [5.32, 5.33], was among the first to use a superposition model to account for two heat transfer mechanisms in boiling heat transfer. The correlation was originally developed for the fully developed saturated boiling and forced-convection vaporization heat transfer regimes. It has been extended to subcooled boiling applications.

For the original saturated boiling correlation, Chen postulated that the heat transfer coefficient was the sum of a contribution due to forced convection plus a contribution due to nucleate boiling. The resulting correlation was considered valid for both the fully-developed nucleate boiling and forced-convection vaporization heat transfer regimes. The postulated superposition model is

$$h_{tp} = h_{ctp} + h_{NB} \qquad \textbf{Eq. 5-66}$$

and the heat flux is

$$q_w = h_{tp}(T_w - T_f) \qquad \textbf{Eq. 5-67}$$

where the fluid temperature is the saturation temperature corresponding to the local pressure.

The heat transfer coefficients for the forced convection component is

$$h_{ctp} = 0.023 Re_{tp}^{0.80} Pr_l^{0.40} \left(\frac{k_l}{D_{hy}} \right) F(X_{tt}) \qquad \textbf{Eq. 5-68}$$

where Re_{tp} is a Reynolds number based on the mass flow rate of the liquid phase and the liquid properties

$$Re_{tp} = \frac{G(1-X)D_{hy}}{\mu_l} \qquad \textbf{Eq. 5-69}$$

where X is the quality. Pr_l is the Prandtl number for the liquid, and the enhancement factor, $F(X_{tt})$, is a function of the Martinelli parameter

$$X_{tt} = \left(\frac{1-X}{X}\right)^{0.90}\left(\frac{\rho_v}{\rho_l}\right)^{0.50}\left(\frac{\mu_l}{\mu_v}\right)^{0.10} \qquad \textbf{Eq. 5-70}$$

Note that the Prandtl number in Eq. 5-68 is the Prandtl number for the liquid and the thermal conductivity of the liquid is used in the (k_l/D_{hy}) factor from the Nusselt number. For the original Chen correlation for saturated boiling all these liquid properties correspond to the properties of the saturated liquid.

It is very important to note that the wetted equivalent diameter, D_{hy}, is used in the equations given above. It is not clear, however, that the wetted equivalent diameter is the best choice to represent the characteristic dimension for rod arrays.

The heat transfer coefficient for the nucleate boiling component is

$$h_{NB} = 0.00122\left[\frac{k_l^{0.79}Cp_l^{0.45}\rho_l^{0.49}}{\sigma^{0.5}\mu_l^{0.29}h_{fg}^{0.24}\rho_v^{0.25}}\right](\Delta T)_{wSAT}^{0.24}(\Delta P)_{SAT}S(Re_{tp}) \qquad \textbf{Eq. 5-71}$$

where $S(Re_{tp})$ is a suppression factor which accounts for the effects of the convection on the boiling process at the clad surface. Also

$$(\Delta T)_{wSAT} = T_w - T_{SAT} \qquad \textbf{Eq. 5-72}$$

and

$$(\Delta P)_{SAT} = P_{SAT}(T_w) - P_{SAT}(T_f) \qquad \textbf{Eq. 5-73}$$

The forced convection component, Eq. 5-68, is based on the Dittus-Boelter correlation and the nucleate boiling component Eq. 5-71 on a pool boiling correlation by Forster and Zuber.

The factor $F(X_{tt})$ in the forced convection contribution is a enhancement factor accounting for improvement in forced convection heat transfer due to vapor generation at the surface.

The factors $F(X_{tt})$ and $S(Re_{tp})$ were originally given by Chen in graphical form. Collier [5.22] has given these as algebraic functions of X_{tt}. and Re_{tp}, respectively

$$F(X_{tt}) = 1 \qquad \text{for} \frac{1}{X_{tt}^{0.10}} \le 0.10 \qquad \textbf{Eq. 5-74}$$

$$F(X_{tt}) = 2.35\left(0.213 + \frac{1}{X_{tt}}\right)^{0.736} \qquad \text{for} \frac{1}{X_{tt}^{0.10}} > 0.10 \qquad \textbf{Eq. 5-75}$$

and

$$S(Re_{tp}) = \frac{1}{(1 + 2.56 \text{x} 10^{-6}\, Re_{tp}^{1.17})} \qquad \textbf{Eq. 5-76}$$

Additionally, Chen [5.33], using the Reynolds analogy, derived the expression

$$F(X_{tt}) = (\Phi_l^2)^{0.444} \qquad \textbf{Eq. 5-77}$$

where the two-phase friction multiplier is

$$\Phi_l^2 = 1 + \frac{20}{X_{tt}} + \frac{1}{X_{tt}^2} \qquad \textbf{Eq. 5-78}$$

and still later extended the analysis to cover liquids with Prandtl number greater than 1.0 to get

$$F(X_{tt}) = \left[\left(\frac{Pr_l + 1}{2}\right)\Phi_l^2\right]^{0.444} \qquad \textbf{Eq. 5-79}$$

The correlation was adapted to subcooled boiling, (Collier references personal communications with Butterworth [5.22]), based on the postulate that the *surface heat flux* is the sum of nucleate boiling plus forced convection components as in Eq. 5-58.

For subcooled boiling the Chen correlation is

$$q_w = h_c(T_w - T_f(Z)) + h_{NB}(T_w - T_{SAT}) \qquad \textbf{Eq. 5-80}$$

For bulk subcooled conditions, based on the assumption that the little vapor generation occurring has negligible effect, the forced convection contribution, Eq. 5-68, is evaluated with $F(X_{tt})$ set to unity. The nucleate boiling contribution, Eq. 5-71, is evaluated by using the single-phase liquid Reynolds number, i.e. X=0.0, in the suppression factor.

The Chen correlation has been the subject of many validation exercises and much information can be found in the literature about its performance compared to experimental data. It is typically used as the benchmark when new correlations are developed. Collier and Thome [5.22] show the performance of the Chen correlation compared to several others, including the Schrock-Grossman correlation [5.34, 5.35, 5.36]. Additionally, Gungor and Winterton, when developing new correlations [5.37, 5.38, 5.39] usually show the performance of the Chen compared with performance of the new correlations. Other validations of the Chen correlation have been given by Shah [5.40, 5.41, 5.42] and Kandlikar [5.43, 5.44, 5.45]. Generally, the newer correlations predict experimental data better than the Chen correlation.

Winterton and Co-Workers Correlations. Winterton and his co-workers have presented three correlations for forced convection boiling. The first correlation [5.37] was developed for both fully developed subcooled and saturated nucleate boiling, The second [5.38] was a simplified and improved version of the original correlation specialized for saturated boiling. And the third correlation [5.39] was an improved version of the original correlation applicable to both subcooled and saturated nucleate boiling.

These workers have compiled an extensive database of forced convection boiling heat transfer data for model and correlation development. The database contains over 4200 points for saturated boiling and about 1000 points for subcooled boiling. The data cover wide ranges of fluids and fluid states for flows in round tubes and annuli. Both unilaterally and bilaterally heated annuli are included as are data from vertical and horizontal test sections. The fluids include water, refrigerants, and cryogenics.

The ranges of conditions for the data are summarized in the following table.

Parameter	Low	High	Units	Low	High	Units
Pressure	0.59	202.6	bar	8.557	2938.308	psia
Diameter	2.95	32.0	mm	0.116	1.26	inches
Mass Flux	12.4	8179.3	kg/m^2 s	9142.5	6030592.95	Lbm/ft^2 hr
Heat Flux	348.9	2.62×10^6	W/m^2	110.6	830278.0	Btu/ft^2 hr
Wall Superheat	0.20	62.30	C	0.360	112.14	F
Fluid Subcooling	0.10	173.70	C	0.180	312.66	F

The Reynolds number, based on the entire mass flow as liquid, ranged from 568.9 to 8.75×10^5 and the liquid Prandtl number ranged from 0.83 to 9.1. The quality ranged from 0.0 to 0.95, but the data at the highest quality were not predicted by any of the correlations examined and were thus omitted for comparisons and correlation development.

In the last paper, [5.39], the authors use the heated equivalent diameter, D_{he}, for the annuli data and state that all the correlations that they compared with the data gave better results when this characteristic diameter has used in place of the wetted equivalent diameter, D_{hy}.

The authors did not use a criterion for ONB; all the data for which the wall temperature was greater than the saturation temperature were considered to be boiling data.

The general form of the correlation given by the authors in Reference 5.39 is different for saturated and subcooled boiling. For saturated boiling, in which the fluid saturation temperature represents the driving potential, the two-phase heat transfer coefficient is

$$h_{tp}^2 = (Fh_l)^2 + (Sh_{NB})^2 \qquad \textbf{Eq. 5-81}$$

where Fh_l is the forced convection contribution and Sh_{NB} is the nucleate boiling contribution. The form of Eq. 5-81 is considered better able to handle the two-phase heat transfer coefficient when only one of the mechanisms dominate.

The forced convection correlation is taken to be given by the Dittus-Boelter correlation

$$h_1 = 0.023(k_l / D_{he}) Re_l^{0.8} Pr_l^{0.4} \qquad \textbf{Eq. 5-82}$$

where the Reynolds number is

$$Re_l = \frac{GD_{he}}{\mu_l} \qquad \textbf{Eq. 5-83}$$

and the Prandtl number is based on the liquid properties. The forced convection enhancement factor, F, is given below. The heat flux in the saturated boiling regime is

$$q_w = h_{tp}(T_w - T_{SAT}) \qquad \textbf{Eq. 5-84}$$

The nucleate boiling correlation is based on the Cooper correlation for pool nucleate boiling

$$h_{NB} = 55.0 P_r^{0.12} q_w^{2/3} (-\log P_r)^{-0.55} M_m^{-0.5} \qquad \textbf{Eq. 5-85}$$

where P_r is the reduced pressure, $P_r = P/P_{crit}$, and M_m is the molar mass of the fluid.

The forced convection enhancement factor was estimated from the data to be

$$F = \left[1 + X\left(\frac{\rho_l}{\rho_v} - 1\right)\right]^{0.35} \qquad \textbf{Eq. 5-86}$$

where X is the quality. The nucleate boiling suppression factor was also estimated from the data to be

$$S = \frac{1}{(1 + 0.055F^{0.1}\,Re_l^{0.16})}$$ **Eq. 5-87**

If the heated channel is horizontal and the Froude number is less than 0.05, the enhancement and suppression factors should be multiplied by correction factors based on the Froude number. The corrections factors are

$$e_f = Fr^{(0.1-2Fr)}$$ **Eq. 5-88**

for the forced convection enhancement, and

$$e_s = \sqrt{Fr}$$ **Eq. 5-89**

for nucleate boiling suppression.

In subcooled boiling the temperature potential for the forced convection and nucleate boiling contributions are different. The heat transfer coefficient of Eq. 5-81 is replaced by

$$q_w = \sqrt{(Fh_l\Delta T_b)^2 + (Sh_{NB}\Delta T_{wSAT})^2}$$ **Eq. 5-90**

where $\Delta T_b = T_w - T_f$ and ΔT_{wSAT} is the standard nomenclature.

Liu and Winterton summarize the performance of the new correlation and several existing correlations when compared with the experimental data for both subcooled and saturated boiling. Generally, they found that the Chen correlation overpredicts the heat transfer coefficient in the high quality regime and underpredicts in the low quality regime.

For subcooled boiling water data, Liu and Winterton report [5.39] that the new correlation predicts the data with a mean error of 12.9% and an average error of 6.4%. The previous Gungor-Winterton [5.37] correlation had 21.4% and 6.4%, respectively. For saturated boiling water data the new correlation predicted the data with 18.1% mean error and 0.90% average error, about the same performance as the Gungor-Winterton [5.38] simplified saturated boiling correlation.

Gungor and Winterton [5.38] includes several tables that present extensive information about the fluid types, geometry, and parameter ranges of their various sets of test data. The performance of different models is also well characterized by fluid type and parameter groupings. The Gungor and Winterton model presented in this reference does not show the superior performance in all categories of the later Liu and Winterton model.

References

5.1. Neil E. Todreas and Mujid S. Kazimi, “Nuclear Systems I Thermal Hydraulic Fundamentals,” Hemisphere Publishing Corporation, New York, 1990.

5.2. T. Krass and L. Meyer, “Experimental Investigation of Turbulent Transport of Momentum and Energy in a Heated Rod Bundle,” Nuclear Engineering and Design, Vol. 180, pp. 185-206, 1998.

5.3. T. Krass and L. Meyer, “Characteristics of Turbulent Velocity and Temperature in a Wall Channel of a Heated Rod Bundle,” Experimental Thermal and Fluid Sciences, Vol. 12, pp. 75-86, 1996.

5.4. Kye Bock Lee and Ho Cheol Jang, “A Numerical Prediction on the Turbulent Flow in Closely Spaced Bare Rod Arrays by a Nonlinear k-e Model,” Nuclear Engineering and Design, Vol. 172, pp. 351-357, 1997.

5.5. L. Meyer, “Measurements of Turbulent Velocity and Temperature in a Central Channel of a Heated Rod Bundle,” Nuclear Engineering and Design, Vol. 146, pp. 71-82, 1994.

5.6. S. V. Moller, “On Phenomena of Turbulent Flow Through Rod Bundles,” Experimental Thermal and Fluid Sciences, Vol. 4, pp. 25-35, 1991.

5.7. S. V. Moller, “Single-Phase Turbulent Mixing in Rod Bundles,” Experimental Thermal and Fluid Sciences, Vol. 5, pp. 26-33, 1992.

5.8. K. Rehme, “Experimental Observations of Turbulent Flow Through Subchannels of Rod Bundles,” Experimental Thermal and Fluid Sciences, Vol. 2, pp. 341-349, 1989.

5.9. X. Wu and A. C. Trupp, “Experimental Study on the Unusual Turbulence Intensity Distributions in Rod-to-Wall Gap Regions,” Experimental Thermal and Fluid Sciences, Vol. 6 (No. 4), pp. 360-370, 1993.

5.10. The RELAP5 Code Development Team, RELAP5/MOD3.2 Code Manual Volume VI: Models and Correlations, NUREG/CR-5535, Vol. 4, 1995.

5.11. H. Schlichting, “Boundary-Layer Theory,” Sixth Edition, McGraw-Hill Book Company, New York, 1968.

5.12. W. M. Kays, “Convective Heat and Mass Transfer,” McGraw-Hill, Inc., New York, 1966.

5.13. W. M. Kays and M. E. Crawford, “Convective Heat and Mass Transfer,” Third Edition, McGraw-Hill, Inc., New York, 1993.

5.14. W. M. Kays and E. Y. Leung, "Heat Transfer in Annular Passages - Hydrodynamically Developed Turbulent Flow with Arbitrarily Prescribed Heat Flux," International Journal of Heat and Mass Transfer, Vol. 6, pp. 537-557, 1962.

5.15. B. S. Petukhov and V. N. Popov, "Theoretical Calculations of Heat Exchange in Turbulent Flow in Tubes of an Incompressible Fluid with Variable Physical Properties," High Temperature, Vol. 1, No. 1, pp. 69-83, 1963.

5.16. B. S. Petukhov, "Heat Transfer and Friction in Turbulent Pipe Flow with Variable Physical Properties," Advances in Heat Transfer, Volume 6, James P. Harnett and Thomas F. Irvine, Jr., eds., Academic Press, New York, 1970.

5.17. B. S. Petukhov and L. I. Roizen, "Generalized Dependencies for Heat Transfer in Tubes of Annular Cross Section," High Temperature, Vol. 12, No. 3, pp. 485-489, 1974.

5.18. P. L. Maksin, B. S. Petukhov and A. F. Polyakov, "Calculation of Turbulent Momentum and Heat Transfer in Pipe Flow of a Gas with Variable Physical Properties," High Temperature, Vol. 15, No. 5, pp. 861-868, 1977.

5.19. V. Gnielinski, "New Equations for Heat and Mass Transfer in Turbulent Pipe and Channel Flow," International Chemical Engineer, Vol. 16, pp. 1907-1920, 1976.

5.20. Vedat S. Arpaci, "Microscales of Turbulence: Heat and Mass Transfer Correlations," Gordon and Breach Science Publishers, Overseas Publishers Association, Amsterdam, 1997.

5.21. M. Dalle and E. Meerwald, "Heat Transfer and Friction Coefficients for Turbulent Flow of Air in Smooth Annuli at High Temperatures," International Journal of Heat and Mass Transfer, Vol. 16, pp. 787-809, 1973.

5.22. John. G. Collier and John. R. Thome, Convective Boiling and Condensation, Third Edition, Oxford University Press, Oxford, 1994.

5.23. S. C. Lee and S. G. Bankoff, "A Comparison of Predictive Models for the Onset of Significant Void at Low Pressures in Forced-Convection Subcooled Boiling," KSME International Journal, Vol. 12, No. 3, pp. 504-513, 1998.

5.24. Van P. Carey, Liquid-Vapor Phase-Change Phenomena, Taylor & Francis, Bristol, PA, 1992.

5.25. P. B. Whalley, Boiling Condensation and Gas-Liquid Flow, Oxford University Press, Oxford, 1987.

5.26. Y. Y. Hsu, "On the Range of Active Nucleation Cavities on a Heating Surface," Transactions of the ASME, Journal of Heat Transfer, Vol. 84, pp. 207-214, 1962.

5.27. A. E. Bergles and W. M. Rohsenow, "The Determination of Forced-Convection Surface-Boiling Heat Transfer," Transactions of the ASME, Journal of Heat Transfer, Vol. 86, pp. 365-372, 1964.

5.28. E. J. Davis and G. H. Anderson, "The Incipience of Nucleate Boiling in Forced Convection Flow," AIChE Journal, Vol. 12, pp. 774-780, 1966.

5.29. W. H. Jens and P. A. Lottes, "Analysis of Heat Transfer, Burnout, Pressure drop, and Density Data for High Pressure Water," Argonne National Laboratory Report, ANL-4627, 1951.

5.30. J. R. S. Thom, W. M. Walker, T. A. Fallon, and G. F. S. Reising, "Boiling in Subcooled Water During Flow up Heated Tubes and Annuli," Presented at the Symposium on Boiling Heat Transfer in Steam Generating Units and Heat Exchangers, Manchester, Sept. 15-16, 1965.

5.31. R. W. Bowring, "Physical Model Based on Bubble Detachment and Calculation of Steam Voidage in the Subcooled Boiling Region of a Heated Channel," OECD Halden Reactor Project Report, HPR-10, 1962.

5.32. J. C. Chen, "A Correlation for Boiling Heat Transfer to Saturated Fluids in Convective Flow," ASME Preprint 63-HT-34 presented at the 6th National Heat Transfer Conference, Boston, August 11-14, 1963.

5.33. J. C. Chen, "A Correlation for Boiling Heat Transfer to Saturated Fluids in Convective Flow," Industrial Engineering and Chemical Process Design and Development, Vol. 5, pp. 322-329, 1966.

5.34. V. E. Schrock and L. M. Grossman, "Forced Convection Boiling Studies," University of California Research Laboratory Report UCRL-13062, 1957.

5.35. V. E. Schrock and L. M. Grossman, "Forced Convection Boiling Studies," in Forced Convection Vaporization Project – Final Report 73308, University of California Research Laboratory Report UCX 2182, November 1959.

5.36. V. E. Schrock and L. M. Grossman, "Forced Convection Boiling in Tubes," Nuclear Science and Engineering, Vol. 12, pp. 474-480, 1962.

5.37. K. E. Gungor and R. H. S. Winterton, "A General Correlation for Flow Boiling in Tubes and Annuli," International Journal of Heat and Mass Transfer, Vol. 29, pp. 351-358, 1986.

5.38. K. E. Gungor and R. H. S. Winterton, "Simplified General Correlation for Saturated Flow Boiling and Comparisons of Correlations with Data," Chemical Engineering Research and Design, Vol. 65, pp. 148-156, 1987.

5.39. Z. Liu and R. H. S. Winterton, "A General Correlation for Saturated and Subcooled Flow Boiling in Tubes and Annuli, Based on a Nucleate Pool Boiling Equation," International Journal of Heat and Mass Transfer, Vol. 34, No. 11, pp. 2759-2766, 1991.

5.40. M. M. Shah, "A General Correlation for Heat Transfer During Subcooled Boiling in Pipes and Annuli," ASHRAE Transactions, Vol. 83, Part 1, pp. 202-215, 1977.

5.41. M. M. Shah, "Generalized Prediction of Heat Transfer During Subcooled Boiling in Annuli," Heat Transfer Engineering, Vol. 4, No. 1, pp. 24-31, 1983.

5.42. M. M. Shah, "Prediction of Heat Transfer During Boiling of Cryogenic Fluids Flowing in Tubes," Cryogenics, Vol. 24. No. 5, pp. 231-236, 1984.

5.43. S. G. Kandlikar, "A General Correlation for Saturated Two-Phase Flow Boiling Heat Transfer Inside Horizontal and Vertical Tubes," Transactions of the ASME Journal of Heat Transfer, Vol. 112, pp. 219-228, 1990.

5.44. S. G. Kandlikar, "Development of a Flow Boiling Map for Subcooled and Saturated Flow Boiling of Different Fluids Inside Circular Tubes," Transactions of the ASME Journal of Heat Transfer, Vol. 113, pp. 190-200, 1991.

5.45. S. G. Kandlikar, "Heat Transfer Characteristics in Partial Boiling, Fully Developed Boiling, and Significant Void Flow Regions of Subcooled Flow Boiling," Transactions of the ASME Journal of Heat Transfer, Vol. 120, pp. 395-401, 1998.

5.46. C.H. Lee, C.J. Chang, S.T. Yin, Y.D. Huang, "Prediction of Incipient Boiling With Forced convective Flow at 0.1 to 20.7 MPa," ASME National Heat Transfer Conference Proceedings, HTD-96, Volume 2, pp. 469-474, 1988.

6
CHARTING THE COURSE TO IMPROVED KNOWLEDGE OF ROD BUNDLE HEAT TRANSFER

The State-of-the-Art

- It has been roughly 40 years since any rod bundle heat transfer tests have been reported in the open literature.
- The rod-array tests which were performed utilized test sections that do not adequately represent the PWR rod bundle geometry (too short and too small of an array). With the instrumentation in these old test sections it is impossible to quantify the bulk flow redistribution that is occurring through the test section. Hence, the effect of a rod-array geometry on the convective heat transfer becomes homogenized with a variety of hydraulic and thermal entrance effects. The results from these tests exhibit significant scatter and provide no consistent information regarding heat transfer in this geometry. No data is available for a prototypical PWR rod bundle geometry and operating conditions that can be used to develop improved heat transfer coefficient correlations.
- Significant uncertainties exist in the accuracy of all available correlations for the convection and subcooled boiling heat transfer processes important to deposition on PWR fuel rods.
- There is no data and no basis for subcooled boiling models in a rod array that includes fluid conditions typical of PWR operation. While some subcooled boiling models include terms for convection and nucleation, the fraction of the surface heat flux that is generating vapor, from the location of onset of nucleation through fully developed subcooled boiling, is an arbitrary allocation based on the researcher's effort to fit the measurements.
- Heat transfer data and correlations in the presence of typical PWR operating chemicals are not available. Data and correlations applicable to the clad surface after deposition has changed the surface characteristics are also not available.

Charting the Course to Improved Rod Bundle Heat Transfer Models

- In view of the above, an experimental program is required to obtain the necessary data to construct models and correlations for heat transfer in rod bundles. The experimental program should be performed with typical PWR geometry and grid designs, at PWR operating conditions, with typical chemical additives.
- Measuring the necessary heater rod and subchannel parameters in a rod-array geometry at PWR pressures and temperatures is a difficult proposition. Furthermore, performing a test in a rod array that provides information on the vapor generation in highly subcooled bulk flows will be particularly difficult at typical PWR operating pressure and flow velocity.

- A key aspect of any new experimental studies must be an assessment of the accuracy that can be accomplished using modern instrumentation. The design of the test array and facility must be such that the scatter is sufficiently small so as not to overshadow potential improvements.
- The subcooled forced convection models of Kays and Petukov offer an improved fundamental structure relative to the traditional Dittus-Boelter equation. This could form the basis for a new rod-array convective heat transfer model.

Summary

The only realistic way to improve the knowledge of heat transfer in PWR open lattice rod arrays is through prototypical testing. Making compromises in the kind of tests that are performed may quite likely leave the state-of-the-art in much the same condition as it is currently. Performing a comprehensive test with top quality instrumentation can provide improved thermal-hydraulic information which will allow the design and operation of fuel cycles with a minimum of economic impact from concerns of developing an adverse axial offset or deposits that may cause fuel failures.

A
CORETRAN ANALYSIS OF THE BATTELLE ROD BUNDLE HEAT TRANSFER TESTS

Introduction

The work presented in the following two references forms a substantial part of the basis for the widely used Weisman [A.1] model for the Colburn coefficient for rod bundles.

D. A. Dingee, W. B. Bell, J. W. Chastain, and S. L. Fawcett, "Heat Transfer from Parallel Rods in Axial Flow," Battelle Memorial Institute Report BMI-1026, 1955. [A.2]

D. A. Dingee and J. W. Chastain, "Heat Transfer from Parallel Rods in Axial Flow," Reactor Heat Transfer Conference of 1956, New York, Book 1, p.462. [A.3]

This Appendix presents an analysis of the Battelle test using the EPRI program CORETRAN [A.4]. The CORETRAN program provides a subchannel analysis capability which can simulate the axial and transverse flow distribution in each channel of the test section and determine the fluid temperature in each channel.

Summary of Test

Dingee and Chastain experimentally examined the convective heat transfer and friction factors using a 3x3 array of 0.5 inch (12.7 mm) outside diameter tubes 23.75 inches (0.603 m) long in both square and triangular pitch arrangements. Only the central rod contained temperature instrumentation, and the subchannel flows and fluid temperature were not measured. Pitch-to-diameter (P/D) ratios of 1.12, 1.2, and 1.27 were tested. The experiments were conducted with water as the working fluid with a Prandtl number of 1.18 and 1.75 at the inlet, over a range of Reynolds numbers from 30,000 to 700,000. The Prandtl number decreases as the water is heated in the test section. The authors reference two theoretical investigations that suggest that thermal and velocity entrance effect are confined to 10 to 15 hydraulic diameters from the inlet.

Dingee presents an analysis of the constituent errors and concludes that the combination of errors would result in an uncertainty of the heat transfer coefficient of approximately 8%.
(See comments that follow in the conclusions sub-section)

The authors examine peripheral variations in the Nusselt number around an instrumented rod but conclude that while there appear to be significant variations, they do not find any consistent periodic behavior. The variations are concluded to be on the order of the experimental accuracy.

This conclusion is supported by a special test that placed the instrumented rod into a concentric tube which preserved the flow area for 1.2 P/D ratio array.

The authors conclude that the experimental Nusselt numbers are approximately 20% higher than that predicted by round-tube correlations using the equivalent diameter of a unit cell in the array.

Analysis

CORETRAN models were set up to examine each of the tests reported by Dingee and Chastian. This includes a complete range of Reynolds numbers, three P/D ratios, and two inlet temperatures.

The results of the CORETRAN analysis are presented in several figures. Figures A-1, A-3, and A-5 illustrate the experimental Nusselt number and the Nusselt number using the Dittus-Boelter correlation with the local conditions from the CORETRAN model. In Figures A-2, A-4, and A-6 an entrance effect model for tubes has been applied to the experimental Nusselt Number.

The following entrance model from Todreas and Kazimi [A.5] credited to Latzko was used.

$$\overline{Nu} = 1.11\left[\frac{\mathrm{Re}^{0.2}}{(L/D_e)^{0.8}}\right]^{0.275} Nu_\infty \qquad \text{for } L/D_e < 0.693 Re^{0.25} \qquad \textbf{Eq. A-1}$$

$$\overline{Nu} = \left[1 + \frac{0.144 Re^{0.25}}{(L/D_e)}\right] Nu_\infty \qquad \text{for } L/D_e > 0.693 Re^{0.25} \qquad \textbf{Eq. A-2}$$

Where Nu_∞ is the reference Nusselt well away from the entrance. A McAdams model which is not a function of Reynolds number was also tested and produced similar results.

There is no reason to believe that the tube entrance effect model is applicable to the rod array, but with the more complex geometry and the bulk flow redistribution which will occur, it should be quite conservative. One would expect that if there were a typical entrance effect in the rod bundle that the experimental Nusselt number at 6 in (0.1524 m) would be larger than at 12 in (0.3048 m), and similarly, the 12 in point would be less than the 18 in (0.4572 m) data point. It is evident from Figures A-1, A-3, and A-5 that there is no such systematic characteristic. Figures A-2, A-4, and A-6 show how much the tube entrance effect model moves the experimental points. The final three figures, Figures A-7, A-8, and A-9, show the adjusted experimental data relative to the Dittus-Boelter correlation using the CORETRAN local conditions. At the P/D of 1.12 the comparison is very well-behaved and the ratio is consistently less than 1.0. At the P/D of 1.20 and 1.27 the scatter and trend becomes pretty unruly. Although there appears to be a trend to larger Nusselt numbers at larger P/D, it seems unreasonable to create a model for the P/D effect from data with such scatter.

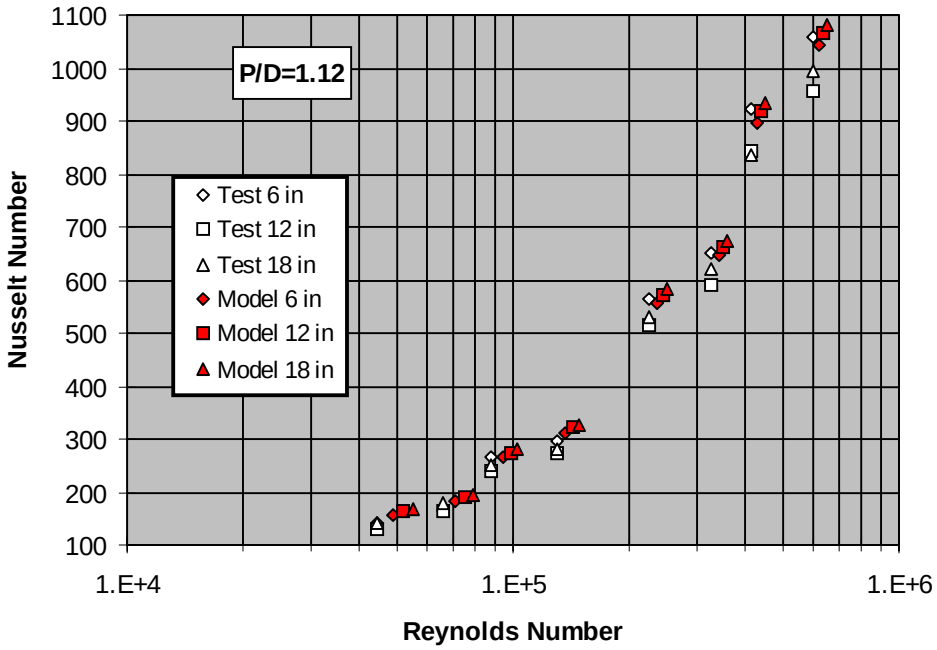

Figure A-1
Predicted & Experimental Nusselt No. at P/D=1.12

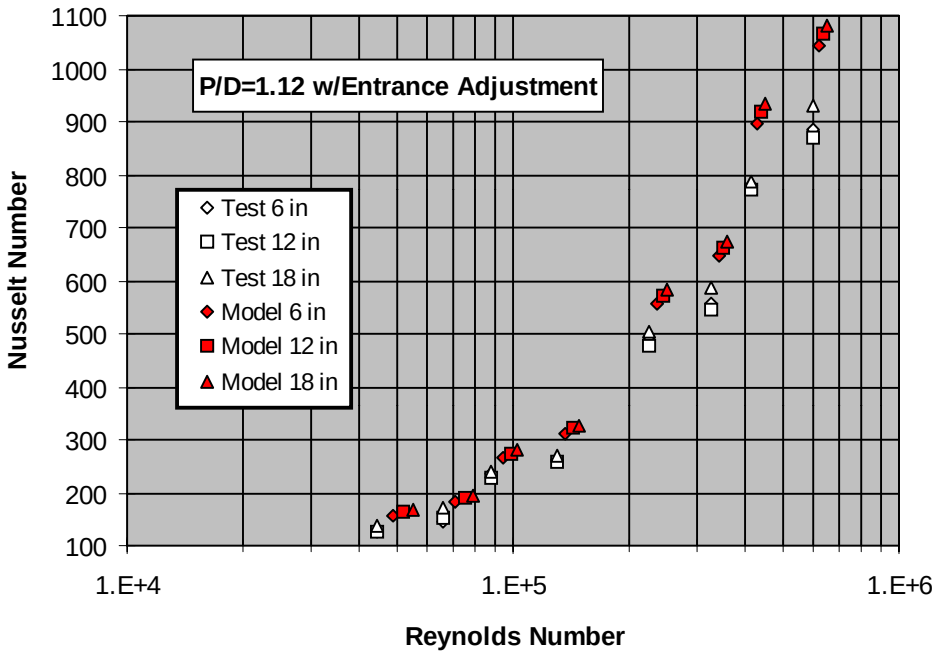

Figure A-2
Predicted & Experimental Nusselt No. at P/D=1.12 W/Entrance Adjustment

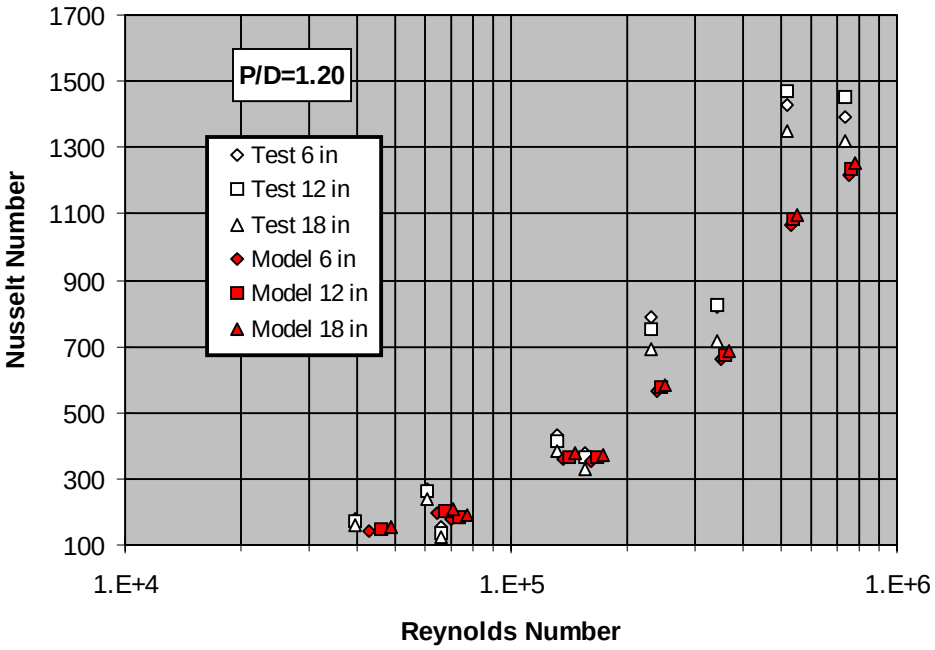

Figure A-3
Predicted & Experimental Nusselt No. at P/D=1.20

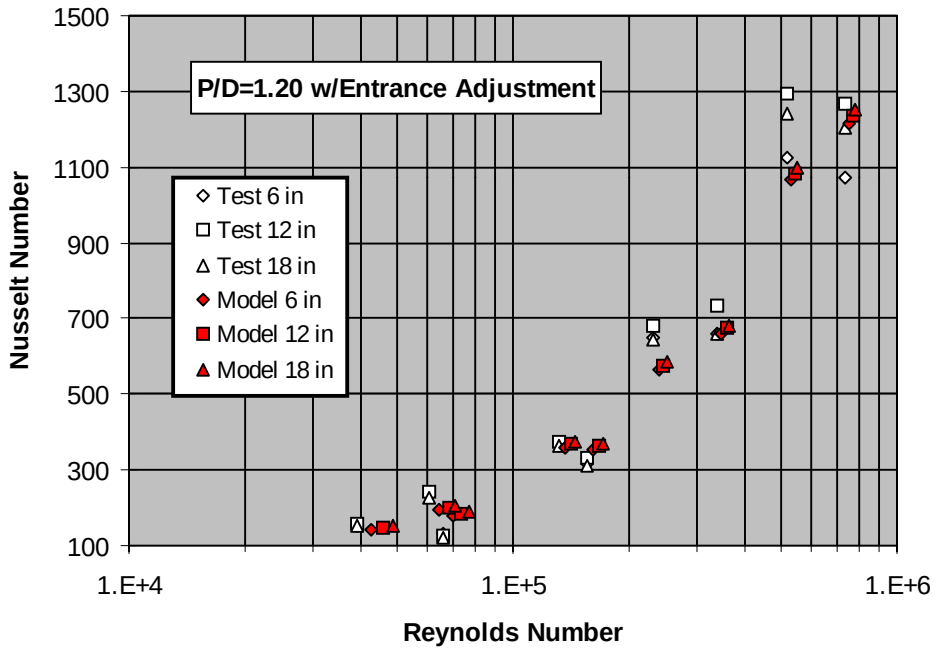

Figure A-4
Predicted & Experimental Nusselt No. at P/D=1.20 W/Entrance Adjustment

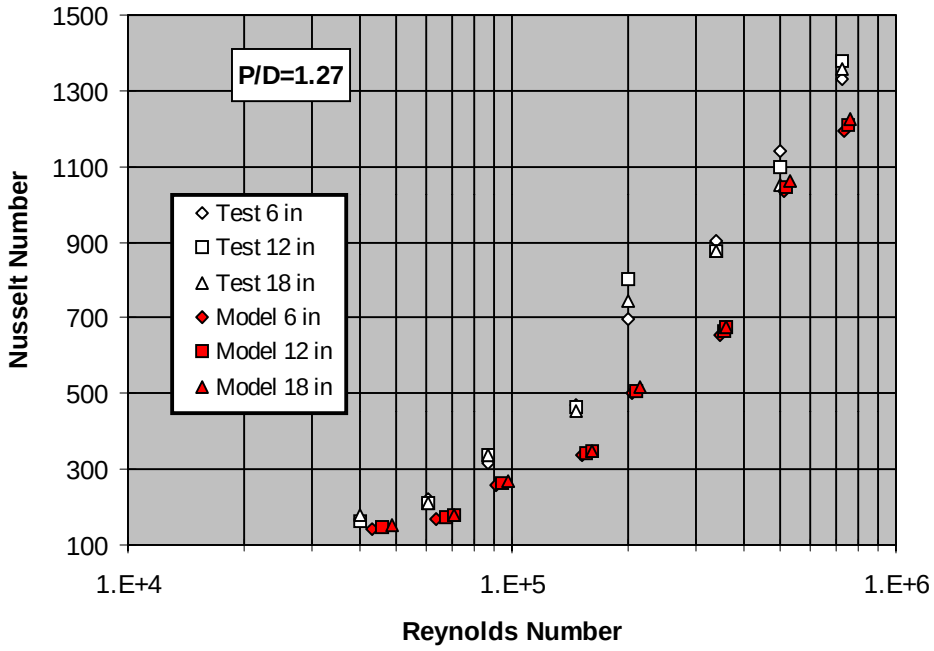

Figure A-5
Predicted & Experimental Nusselt No. at P/D=1.27

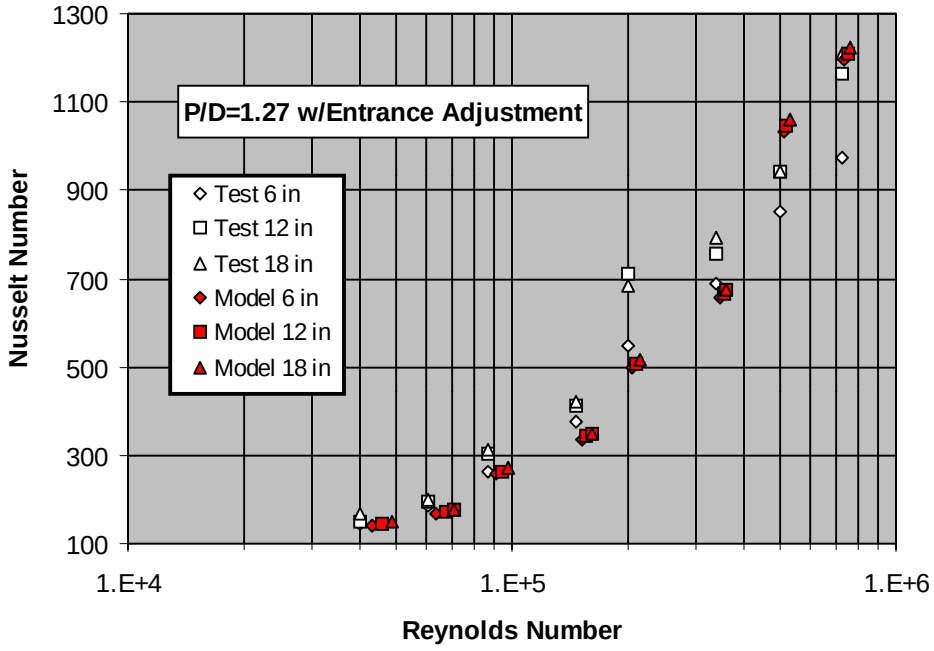

Figure A-6
Predicted & Experimental Nusselt No. at P/D=1.27 W/Entrance Adjustment

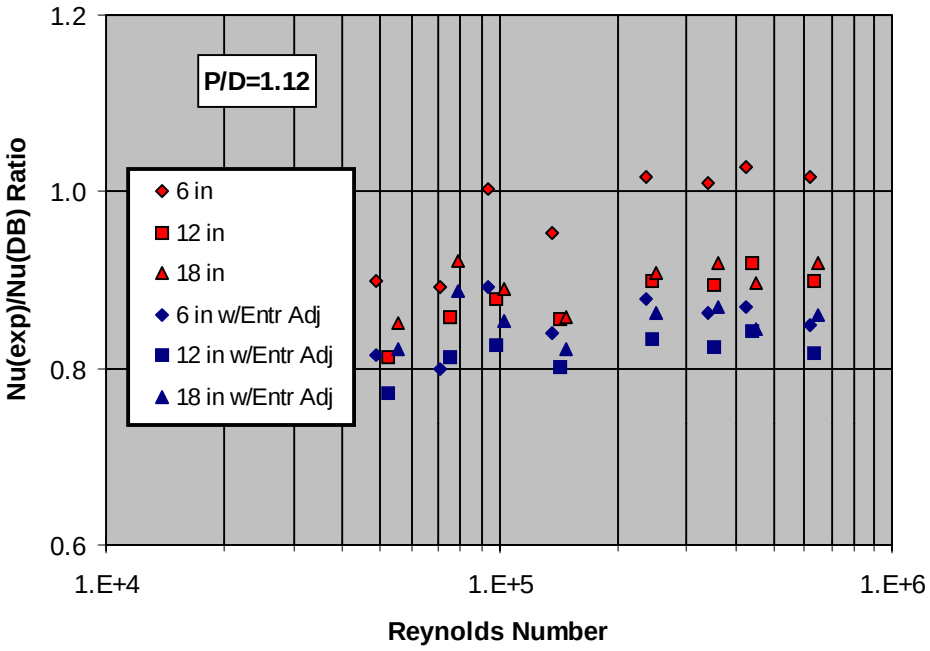

Figure A-7
Ratio of Experimental/Dittus-Boelter Nusselt Number at P/D=1.12

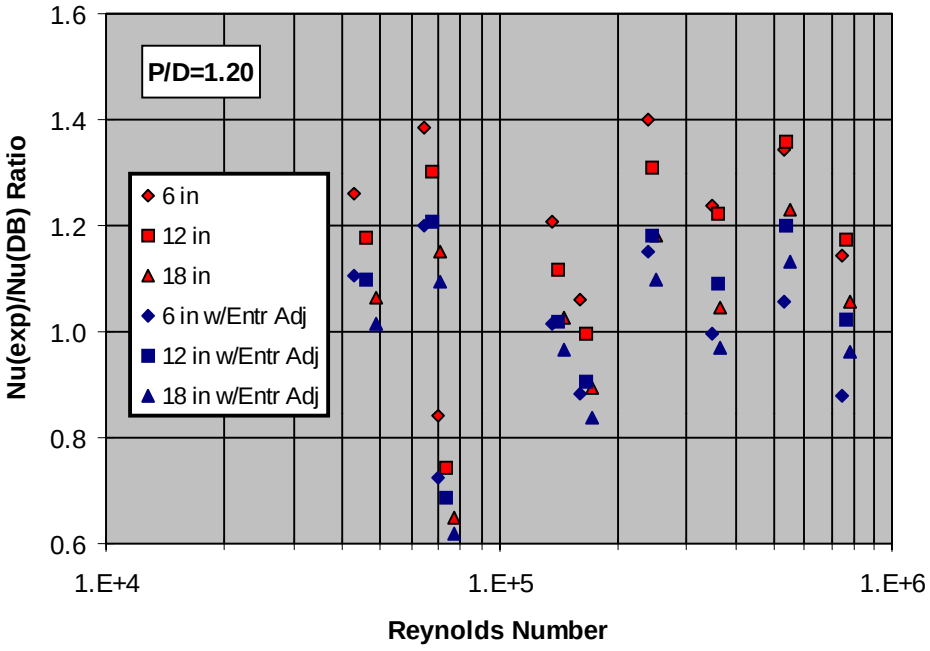

Figure A-8
Ratio of Experimental/Dittus-Boelter Nusselt Number at P/D=1.20

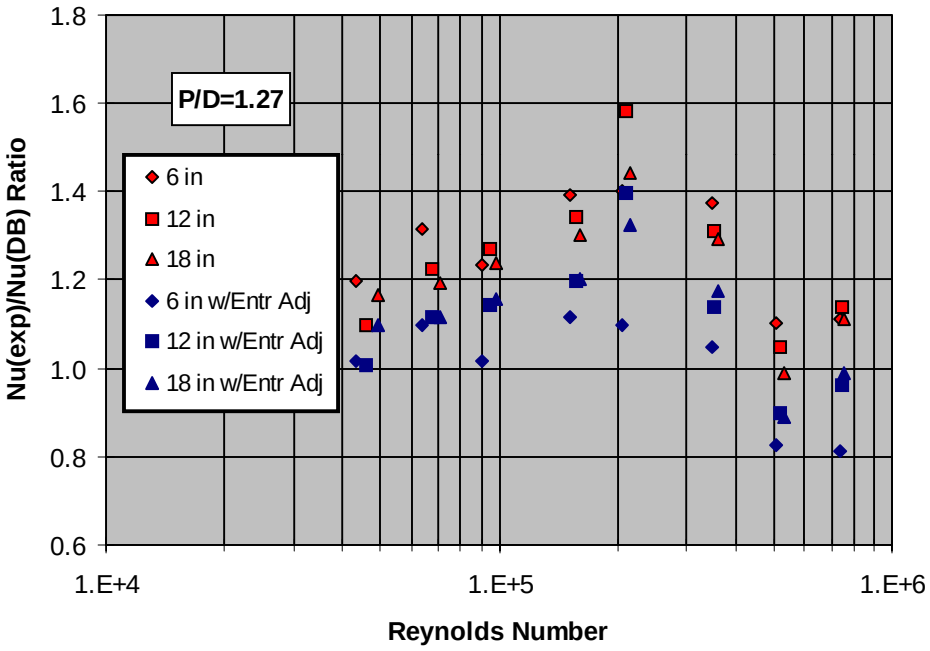

Figure A-9
Ratio of Experimental/Dittus-Boelter Nusselt Number at P/D=1.27

Conclusions

There is substantial bulk flow redistribution occurring throughout the entire length of the 23.75 inch (0.603 m) test section. Measurements were taken at 6, 12, and 18 inches(0.1524, 0.3048, and 0.4572 m). Since cross-flow will impact the turbulence, and thus the heat transfer coefficient, it is impossible to draw a conclusion about the heat transfer behavior of the rod bundle geometry relative to a tube. In essence, there can be no fully developed thermal boundary layer until the channel flow distribution has come to its steady state. The results show substantial scatter and only remote trends.

The higher Reynolds number data points will have a larger measurement error because the film temperature difference is small relative to the errors in measuring the fluid and inside wall temperature. With a constant power, the wall to bulk temperature difference at the low Reynolds numbers is on the order of 31.25°C (50°F), where at the high Reynolds numbers the difference is 4.4 to 6.2°C (7 to 10°F). The quoted accuracy of 8% may be suspect at higher Reynolds numbers.

WARNING: This Document contains information classified under U.S. Export Control regulations as restricted from export outside the United States. You are under an obligation to ensure that you have a legal right to obtain access to this information and to ensure that you obtain an export license prior to any re-export of this information. Special restrictions apply to access by anyone that is not a United States citizen or a Permanent United States resident. For further information regarding your obligations, please see the information contained below in the section titled "Export Control Restrictions."

Export Control Restrictions

Access to and use of EPRI Intellectual Property is granted with the specific understanding and requirement that responsibility for ensuring full compliance with all applicable U.S. and foreign export laws and regulations is being undertaken by you and your company. This includes an obligation to ensure that any individual receiving access hereunder who is not a U.S. citizen or permanent U.S. resident is permitted access under applicable U.S. and foreign export laws and regulations. In the event you are uncertain whether you or your company may lawfully obtain access to this EPRI Intellectual Property, you acknowledge that it is your obligation to consult with your company's legal counsel to determine whether this access is lawful. Although EPRI may make available on a case by case basis an informal assessment of the applicable U.S. export classification for specific EPRI Intellectual Property, you and your company acknowledge that this assessment is solely for informational purposes and not for reliance purposes. You and your company acknowledge that it is still the obligation of you and your company to make your own assessment of the applicable U.S. export classification and ensure compliance accordingly. You and your company understand and acknowledge your obligations to make a prompt report to EPRI and the appropriate authorities regarding any access to or use of EPRI Intellectual Property hereunder that may be in violation of applicable U.S. or foreign export laws or regulations.

About EPRI

EPRI creates science and technology solutions for the global energy and energy services industry. U.S. electric utilities established the Electric Power Research Institute in 1973 as a nonprofit research consortium for the benefit of utility members, their customers, and society. Now known simply as EPRI, the company provides a wide range of innovative products and services to more than 1000 energy-related organizations in 40 countries. EPRI's multidisciplinary team of scientists and engineers draws on a worldwide network of technical and business expertise to help solve today's toughest energy and environmental problems.

EPRI. Electrify the World

SINGLE USER LICENSE AGREEMENT

THIS IS A LEGALLY BINDING AGREEMENT BETWEEN YOU AND THE ELECTRIC POWER RESEARCH INSTITUTE, INC. (EPRI). PLEASE READ IT CAREFULLY BEFORE REMOVING THE WRAPPING MATERIAL.

BY OPENING THIS SEALED PACKAGE YOU ARE AGREEING TO THE TERMS OF THIS AGREEMENT. IF YOU DO NOT AGREE TO THE TERMS OF THIS AGREEMENT, PROMPTLY RETURN THE UNOPENED PACKAGE TO EPRI AND THE PURCHASE PRICE WILL BE REFUNDED.

1. GRANT OF LICENSE

EPRI grants you the nonexclusive and nontransferable right during the term of this agreement to use this package only for your own benefit and the benefit of your organization. This means that the following may use this package: (I) your company (at any site owned or operated by your company); (II) its subsidiaries or other related entities; and (III) a consultant to your company or related entities, if the consultant has entered into a contract agreeing not to disclose the package outside of its organization or to use the package for its own benefit or the benefit of any party other than your company.

This shrink-wrap license agreement is subordinate to the terms of the Master Utility License Agreement between most U.S. EPRI member utilities and EPRI. Any EPRI member utility that does not have a Master Utility License Agreement may get one on request.

2. COPYRIGHT

This package, including the information contained in it, is either licensed to EPRI or owned by EPRI and is protected by United States and international copyright laws. You may not, without the prior written permission of EPRI, reproduce, translate or modify this package, in any form, in whole or in part, or prepare any derivative work based on this package.

3. RESTRICTIONS

You may not rent, lease, license, disclose or give this package to any person or organization, or use the information contained in this package, for the benefit of any third party or for any purpose other than as specified above unless such use is with the prior written permission of EPRI. You agree to take all reasonable steps to prevent unauthorized disclosure or use of this package. Except as specified above, this agreement does not grant you any right to patents, copyrights, trade secrets, trade names, trademarks or any other intellectual property, rights or licenses in respect of this package.

4. TERM AND TERMINATION

This license and this agreement are effective until terminated. You may terminate them at any time by destroying this package. EPRI has the right to terminate the license and this agreement immediately if you fail to comply with any term or condition of this agreement. Upon any termination you may destroy this package, but all obligations of nondisclosure will remain in effect.

5. DISCLAIMER OF WARRANTIES AND LIMITATION OF LIABILITIES

NEITHER EPRI, ANY MEMBER OF EPRI, ANY COSPONSOR, NOR ANY PERSON OR ORGANIZATION ACTING ON BEHALF OF ANY OF THEM:

(A) MAKES ANY WARRANTY OR REPRESENTATION WHATSOEVER, EXPRESS OR IMPLIED, (I) WITH RESPECT TO THE USE OF ANY INFORMATION, APPARATUS, METHOD, PROCESS OR SIMILAR ITEM DISCLOSED IN THIS PACKAGE, INCLUDING MERCHANTABILITY AND FITNESS FOR A PARTICULAR PURPOSE, OR (II) THAT SUCH USE DOES NOT INFRINGE ON OR INTERFERE WITH PRIVATELY OWNED RIGHTS, INCLUDING ANY PARTY'S INTELLECTUAL PROPERTY, OR (III) THAT THIS PACKAGE IS SUITABLE TO ANY PARTICULAR USER'S CIRCUMSTANCE; OR

(B) ASSUMES RESPONSIBILITY FOR ANY DAMAGES OR OTHER LIABILITY WHATSOEVER (INCLUDING ANY CONSEQUENTIAL DAMAGES, EVEN IF EPRI OR ANY EPRI REPRESENTATIVE HAS BEEN ADVISED OF THE POSSIBILITY OF SUCH DAMAGES) RESULTING FROM YOUR SELECTION OR USE OF THIS PACKAGE OR ANY INFORMATION, APPARATUS, METHOD, PROCESS OR SIMILAR ITEM DISCLOSED IN THIS PACKAGE.

6. EXPORT

The laws and regulations of the United States restrict the export and re-export of any portion of this package, and you agree not to export or re-export this package or any related technical data in any form without the appropriate United States and foreign government approvals.

7. CHOICE OF LAW

This agreement will be governed by the laws of the State of California as applied to transactions taking place entirely in California between California residents.

8. INTEGRATION

You have read and understand this agreement, and acknowledge that it is the final, complete and exclusive agreement between you and EPRI concerning its subject matter, superseding any prior related understanding or agreement. No waiver, variation or different terms of this agreement will be enforceable against EPRI unless EPRI gives its prior written consent, signed by an officer of EPRI.

Program:

Nuclear Power

1000215

EPRI • 3412 Hillview Avenue, Palo Alto, California 94304 • PO Box 10412, Palo Alto, California 94303 • USA
800.313.3774 • 650.855.2121 • askepri@epri.com • www.epri.com